A wavelet-based generalization of the multifractal formalism from scalar to vector valued d-dimensional random fields : from theoretical concepts to experimental applications

P. Kestener and A. Arneodo

Laboratoire de Physique
Ecole Normale Supérieure de Lyon
46, allée d'Italie
69364 Lyon cedex 07, FRANCE

Report Documentation Page

Form Approved
OMB No. 0704-0188

1. REPORT DATE **07 JAN 2005**	2. REPORT TYPE **N/A**	3. DATES COVERED **-**

4. TITLE AND SUBTITLE **A wavelet-based generalization of the multifractal formalism from scalar to vector valued d-dimensional random fields : from theoretical concepts to experimental applications**	5a. CONTRACT NUMBER 5b. GRANT NUMBER 5c. PROGRAM ELEMENT NUMBER
6. AUTHOR(S)	5d. PROJECT NUMBER 5e. TASK NUMBER 5f. WORK UNIT NUMBER
7. PERFORMING ORGANIZATION NAME(S) AND ADDRESS(ES) **Laboratoire de PhysiqueEcole Normale Supérieure de Lyon46, allée dItalie69364 Lyon cedex 07, FRANCE**	8. PERFORMING ORGANIZATION REPORT NUMBER
9. SPONSORING/MONITORING AGENCY NAME(S) AND ADDRESS(ES)	10. SPONSOR/MONITOR'S ACRONYM(S) 11. SPONSOR/MONITOR'S REPORT NUMBER(S)

12. DISTRIBUTION/AVAILABILITY STATEMENT
Approved for public release, distribution unlimited

13. SUPPLEMENTARY NOTES
See also ADM001750, Wavelets and Multifractal Analysis (WAMA) Workshop held on 19-31 July 2004., The original document contains color images.

14. ABSTRACT

15. SUBJECT TERMS

16. SECURITY CLASSIFICATION OF:			17. LIMITATION OF ABSTRACT	18. NUMBER OF PAGES	19a. NAME OF RESPONSIBLE PERSON
a. REPORT **unclassified**	b. ABSTRACT **unclassified**	c. THIS PAGE **unclassified**	**UU**	**41**	

2D WTMM Methodology : PhD work of N. Decoster

2D data : I

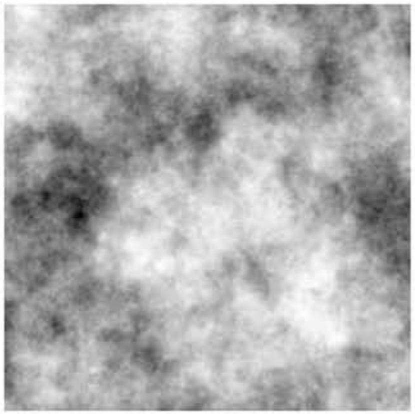

$$\xrightarrow{\text{Smoothing scale } a} \qquad \xrightarrow{\text{Gradient } \nabla}$$

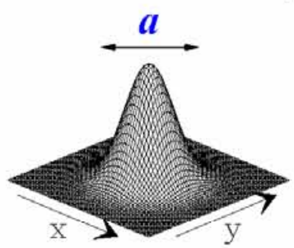

$$\underbrace{\qquad\qquad\qquad \left[\frac{\partial}{\partial x}, \frac{\partial}{\partial y}\right]}_{\text{Wavelet Transform}}$$

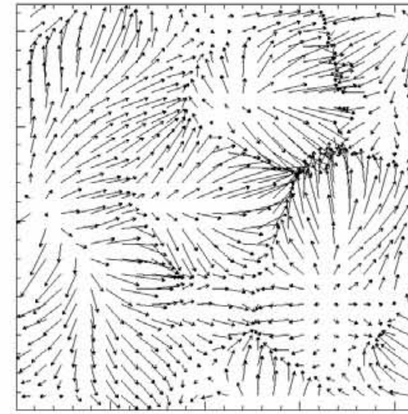

$\downarrow$

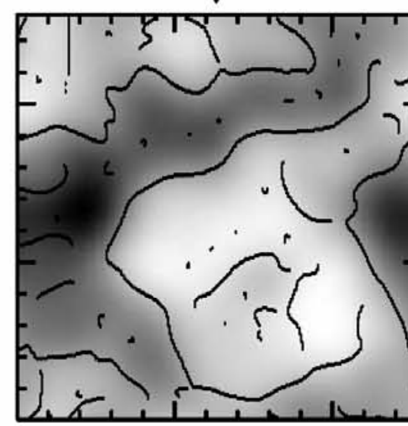

$$\mathbf{T}_{\psi}(\mathbf{r}, a) = \begin{pmatrix} I * \frac{\partial \phi_a}{\partial x}(\mathbf{r}) \\ I * \frac{\partial \phi_a}{\partial y}(\mathbf{r}) \end{pmatrix}$$

$$\mathbf{T}_{\psi}(\mathbf{r}, a) = \nabla (I * \phi_a)(\mathbf{r}) = (\mathcal{M}_{\psi}(\mathbf{r}, a), \mathcal{A}_{\psi}(\mathbf{r}, a))$$

WTMM Methodology : Skeleton

WTMM Chains

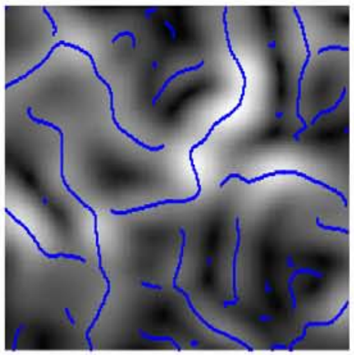

WTMMM

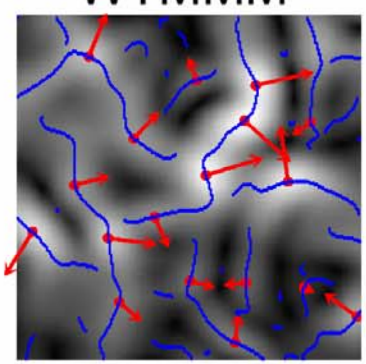

WTMM Chains at 3 different scales

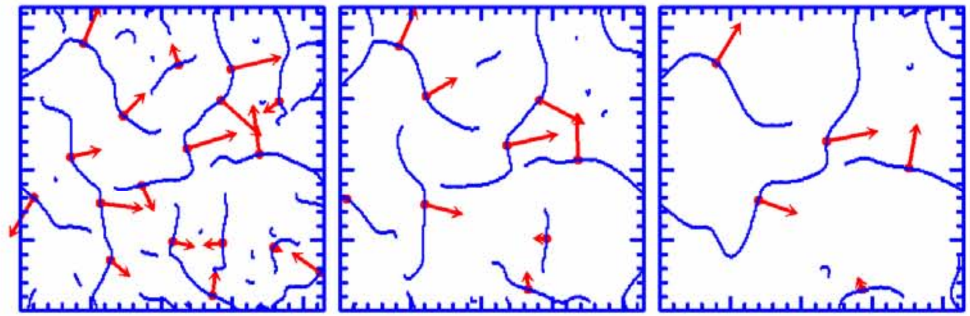

Maxima lines : WT skeleton

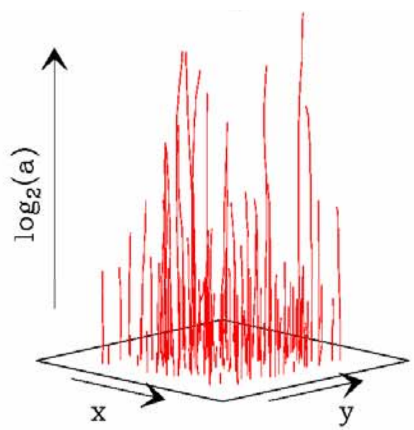

Local roughness characterization : Hölder exponent

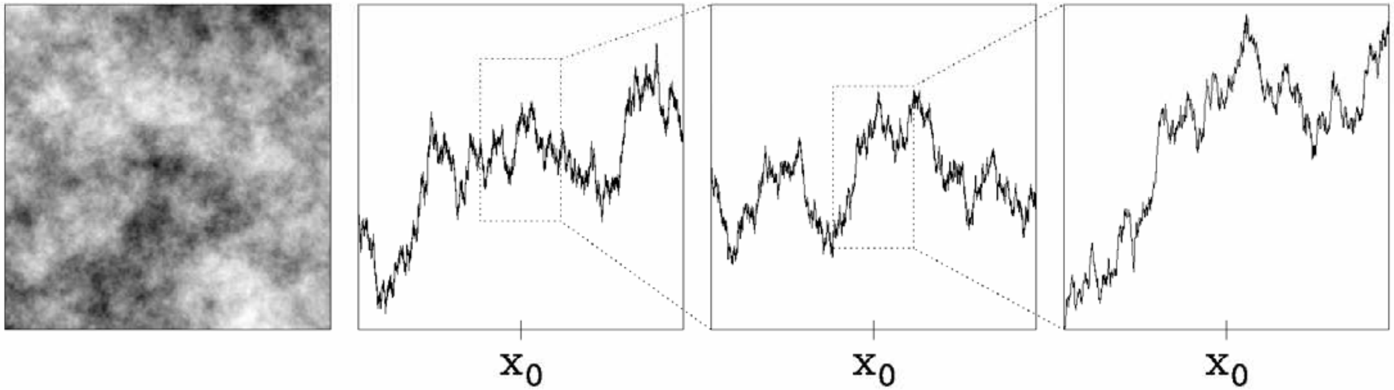

$$f(x_0 + \lambda u) - f(x_0) \sim \lambda^{h(x_0)} (f(x_0 + u) - f(x_0))$$

- **Monofractal Image**
- **Multifractal Image**

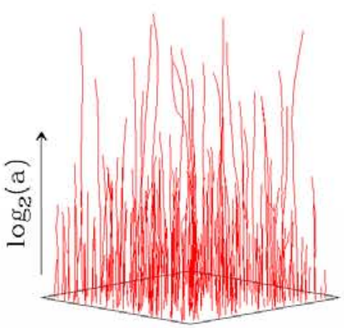

$$\mathcal{M} \sim a^{h},$$

single h

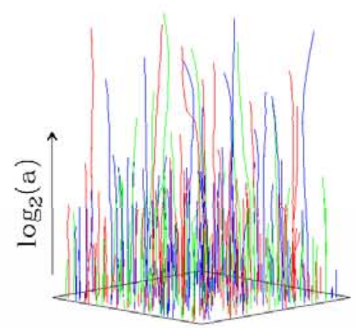

$$\mathcal{M} \sim a^{h}, a^{h}, a^{h},$$

$$h \in [h_{\min}, h_{\max}]$$

WTMM Method : multifractal formalism

Singularity spectrum :

$$D(h) = d_H\{\mathrm{r} \in R^d, h(\mathrm{r}) = h\}$$

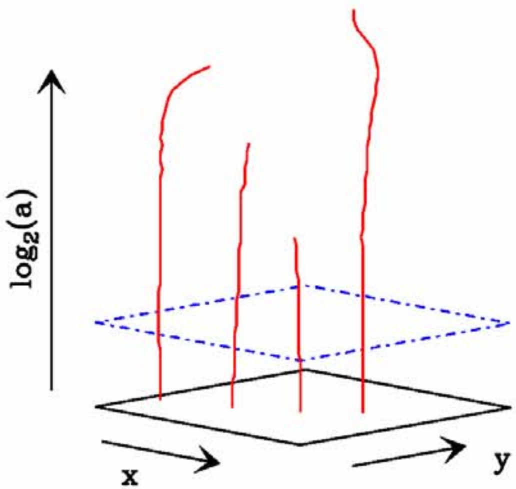

Legendre transform :

$$D(h) = \min_q\big(qh - \tau(q)\big)$$

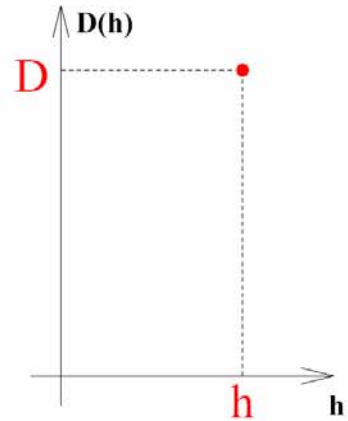

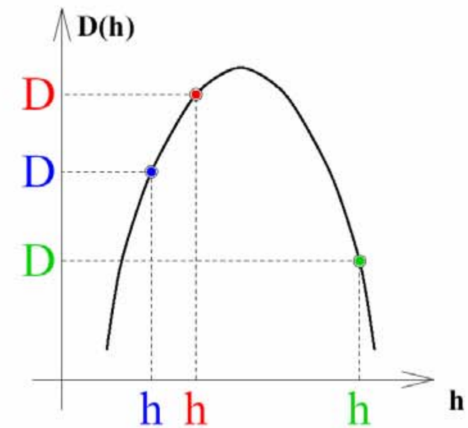

Analogy with statistical physics : compute
partition functions

$$\mathcal{Z}(q,a) = \sum_{\mathcal{L}(a)} \left(\mathcal{M}_\psi(\mathrm{r},a)\right)^q \sim a^{\tau(q)}$$

WTMM Method : multifractal formalism

Singularity spectrum :

$$D(h) = d_H\{\mathrm{r} \in R^d, h(\mathrm{r}) = h\}$$

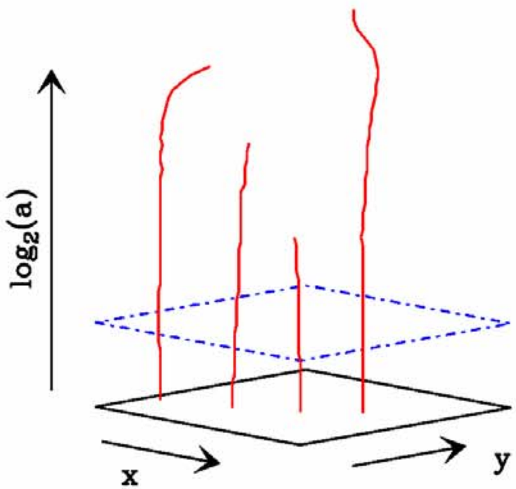

Legendre transform :

$$D(h) = \min_q\big(qh - \tau(q)\big)$$

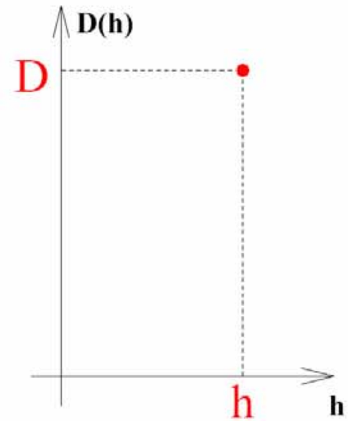

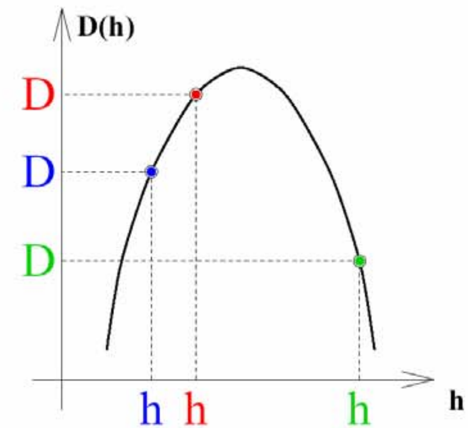

Analogy with statistical physics : compute partition functions

$$\mathcal{Z}(q,a) = \sum_{\mathcal{L}(a)} \left(\mathcal{M}_\psi(\mathrm{r},a)\right)^q \sim a^{\tau(q)}$$

$$\mathcal{H}(q,a) = \sum_{\mathcal{L}(a)} \ln|\mathcal{M}_\psi(\mathrm{r},a)|\, \mathcal{W}_\psi(\mathrm{r},a) \sim a^{h(q)}$$

$$\mathcal{D}(q,a) = \sum_{\mathcal{L}(a)} \ln|\mathcal{W}_\psi(\mathrm{r},a)|\, \mathcal{W}_\psi(\mathrm{r},a) \sim a^{D(q)}$$

Application to synthetic monofractal surfaces

fractional Brownian surfaces : $B_H(\mathrm{r})$

- $H < 0.5$: anti-correlated increments
- $H = 0.5$: uncorrelated increments
- $H > 0.5$: correlated increments

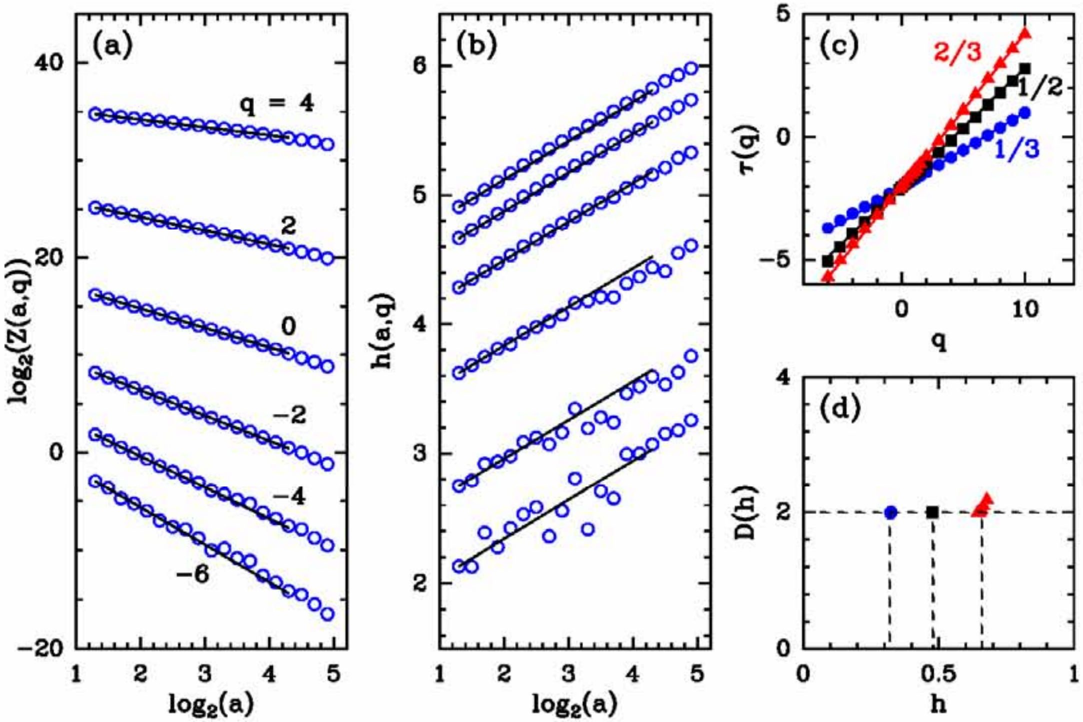

H=1/3

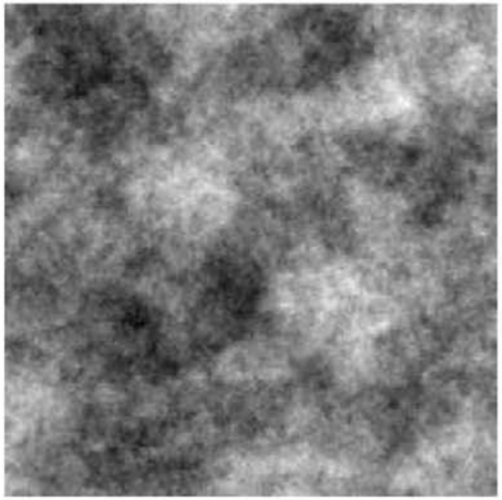

Theoretical Predictions :

- $\tau(q)$ is linear :
  $\tau(q) = qH - 2$
- multifractal spectrum is degenerated :
  $D(h = H) = 2$

Application to synthetic multifractal surfaces

Multifractal (Fractionally Integrated Singular Cascades) surfaces

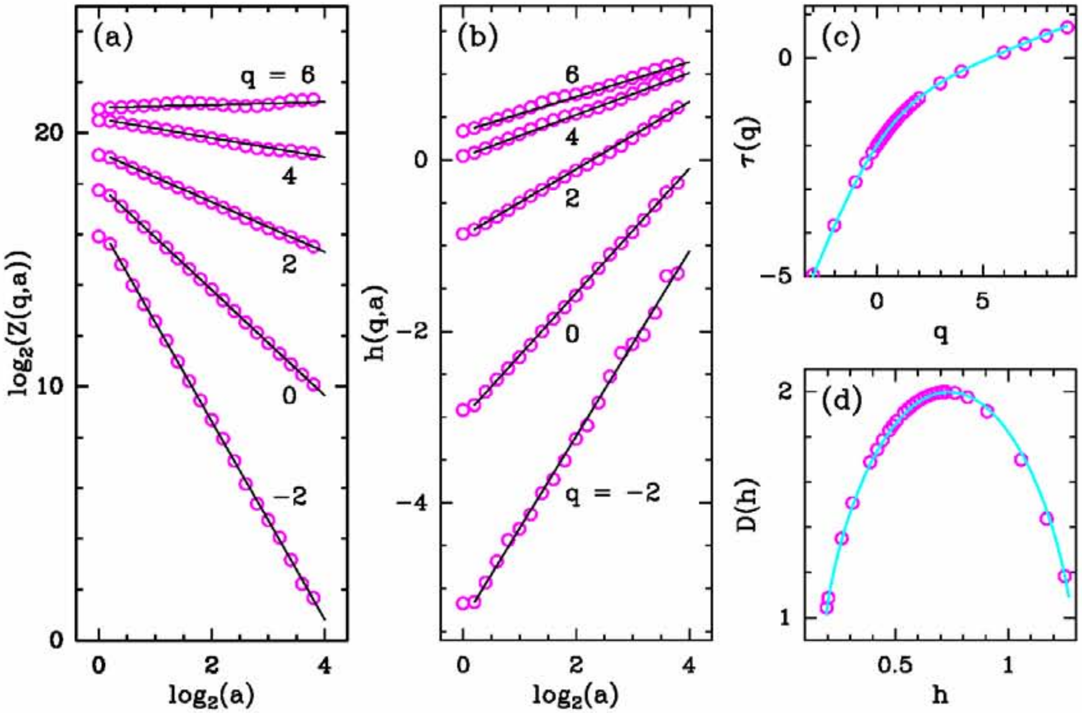

FISC

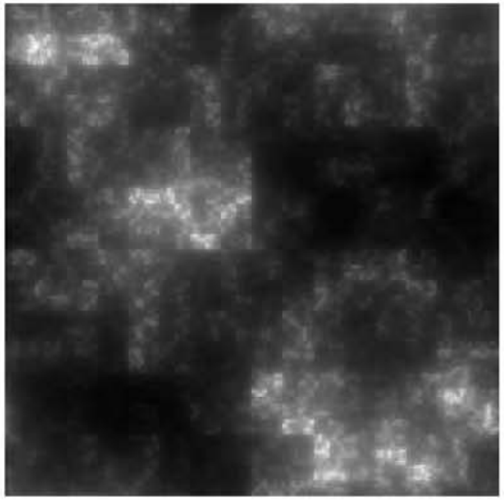

Theoretical predictions :

- $\tau(q)$ is non-linear

$$\tau(q) = -2 - q(1 - H^*) - \log_2(p_1{}^q + p_2{}^q)$$

- singularity spectrum is a non-degenerated convex curve

Mammography and breast anatomy

Goals : using WTMM method to help in diagnosis of breast cancer

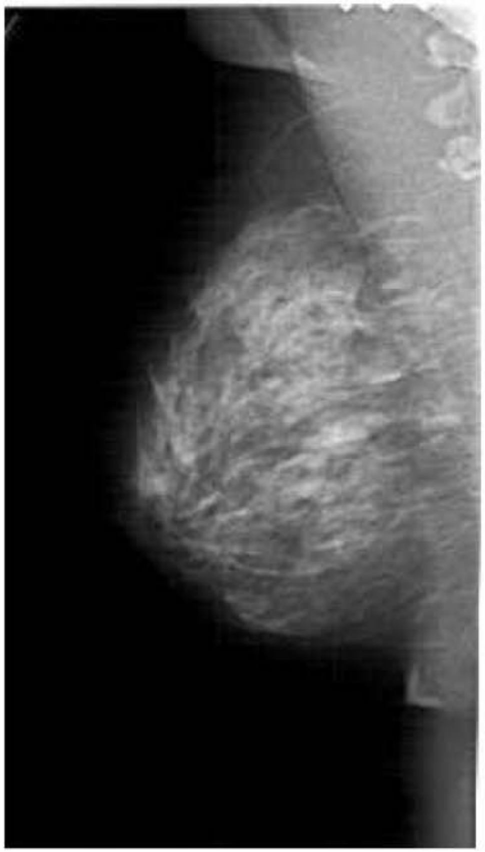

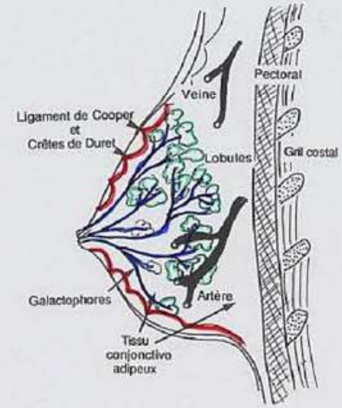

FIG. 1-1 *a. – Anatomie simplifiée.*

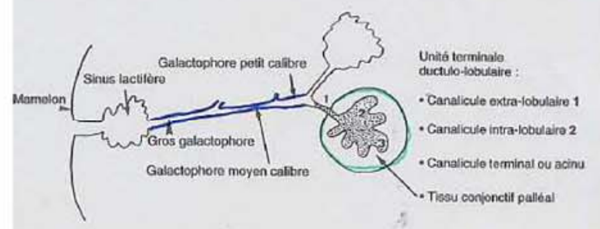

FIG. 1-1 *b. – Unité terminale ductulo-lobulaire, selon Wellings.*

What is breast cancer ?

- malignant tumor of mammal gland
- incidence : 30000 new case each year in France
- prevention is very difficult (as opposed to lung cancer)
- hereditarity : 5 to 10 % only (BRCA1/2 genes)
- forecast depends on the tumoral volume at diagnosis

$\Rightarrow$ **SCREENING** using mammography

Radiological anomalies

Opacities

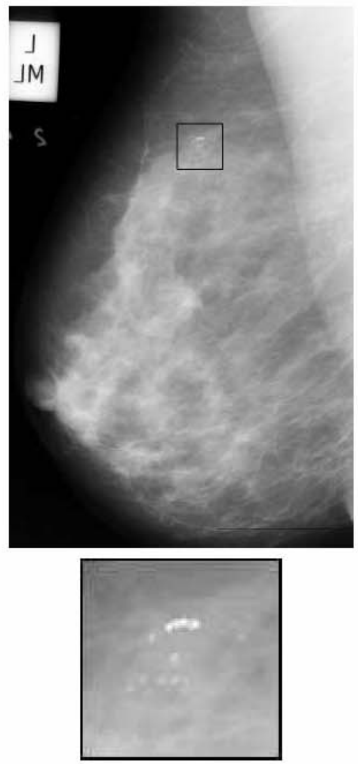

Calcifications

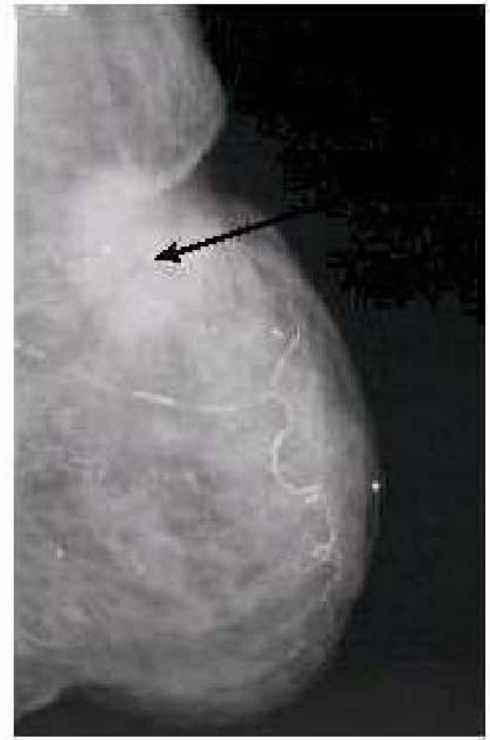

Architectural distortions

Digitalized mammographies : texture analysis

- dense breasts : more difficult to diagnose
- only 2 classes of monofractal properties

Digital Database for Screening Mammography:

http://marathon.csee.usf.edu/Mammography/Database.html

Dense breast

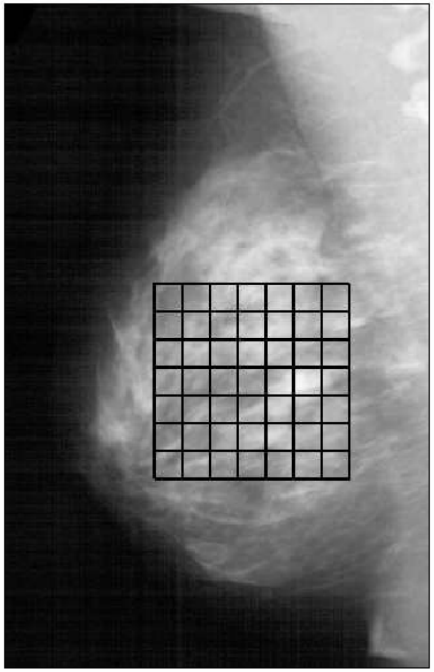

Fatty breast

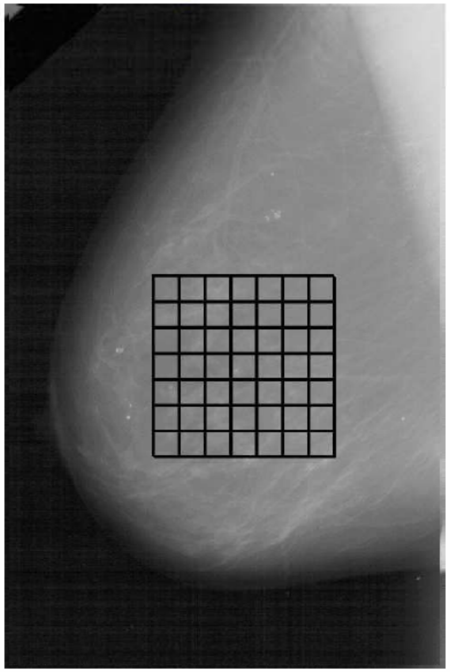

Application of 2D WTMM methodology in mammography

Tissue classifi cation : dense

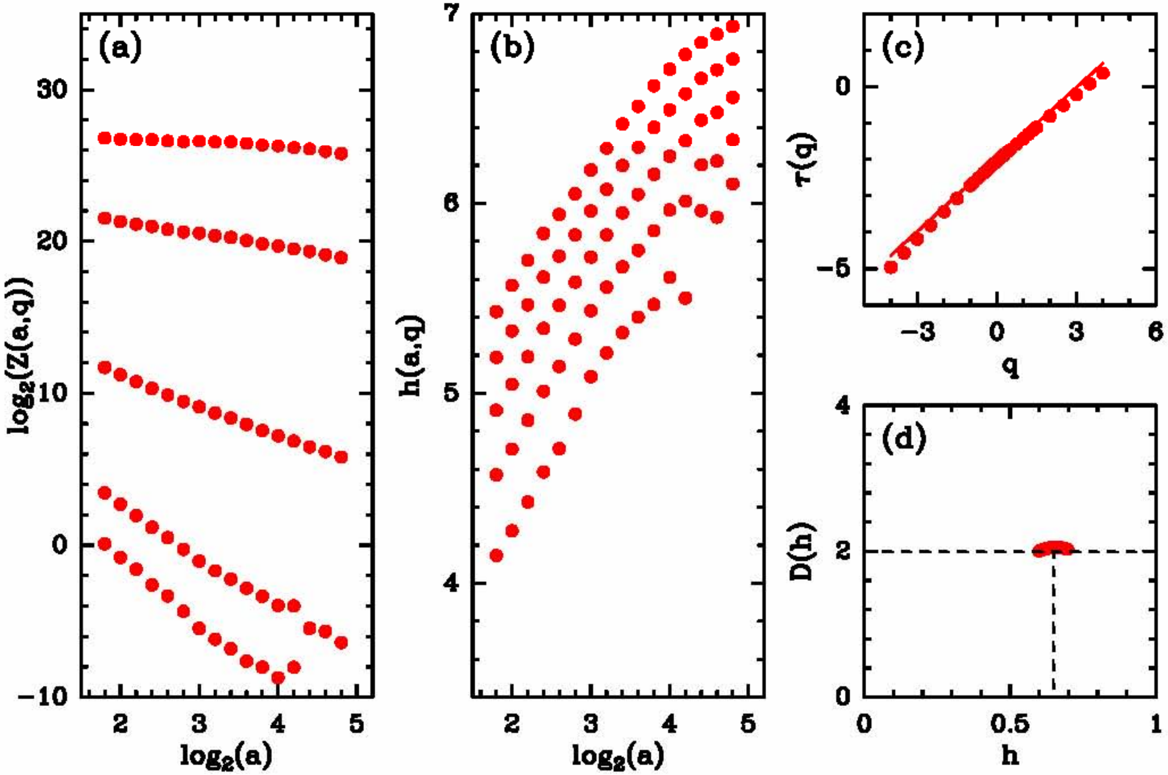

- Dense breast : monofractal, $H = 0.65$ persitent correlations

Application of 2D WTMM methodology in mammography

Tissue classification : dense vs fatty

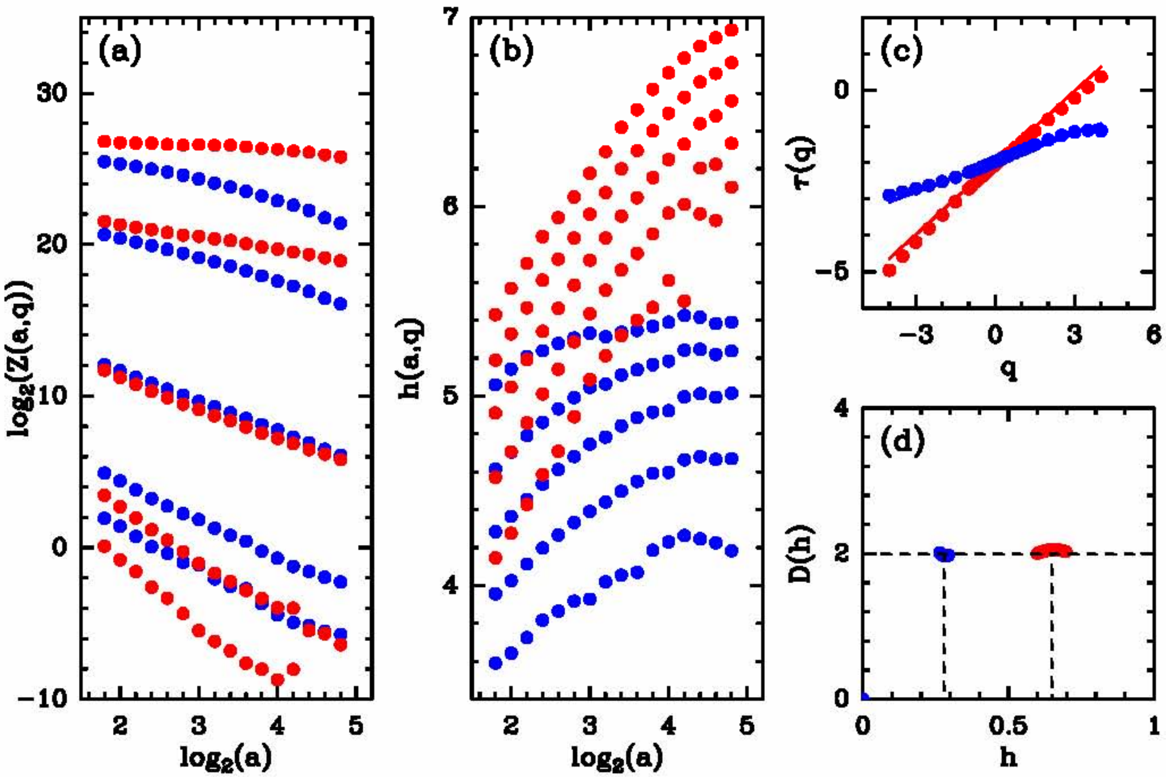

- **Dense** breast :
  monofractal, $H = 0.65$
  persitent correlations
- **Fatty** breast :
  monofractal, $H = 0.30$
  anti-persitent correlations

Application to digitalized mammographies

Colored Maps :
segmentation of dense $h > 0.52$ areas and fatty $h < 0.38$ areas

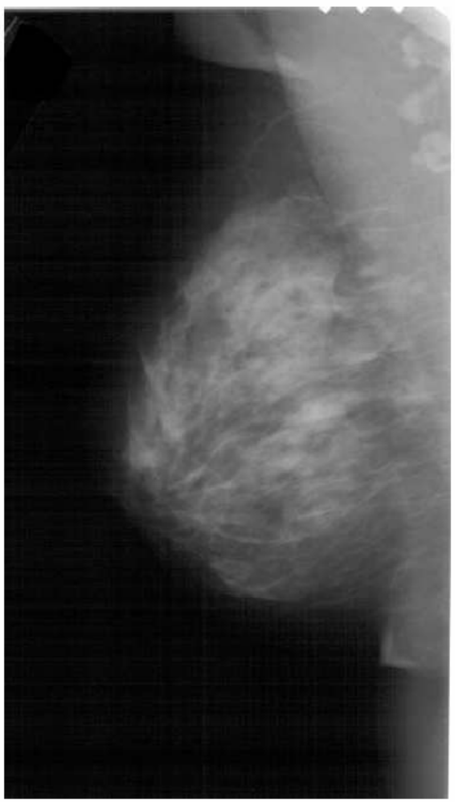

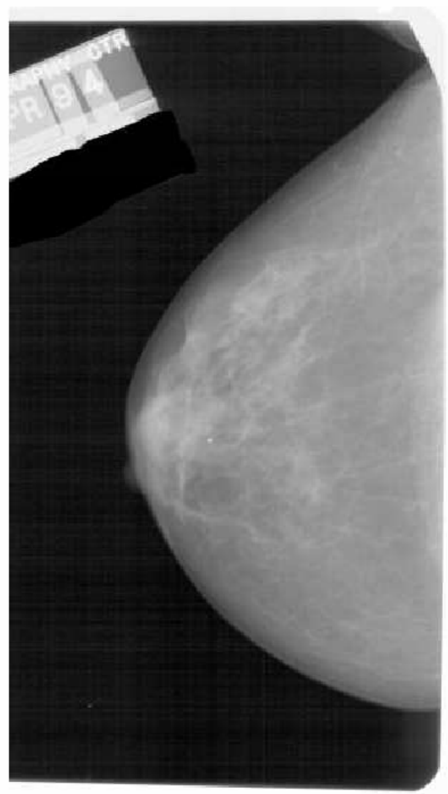

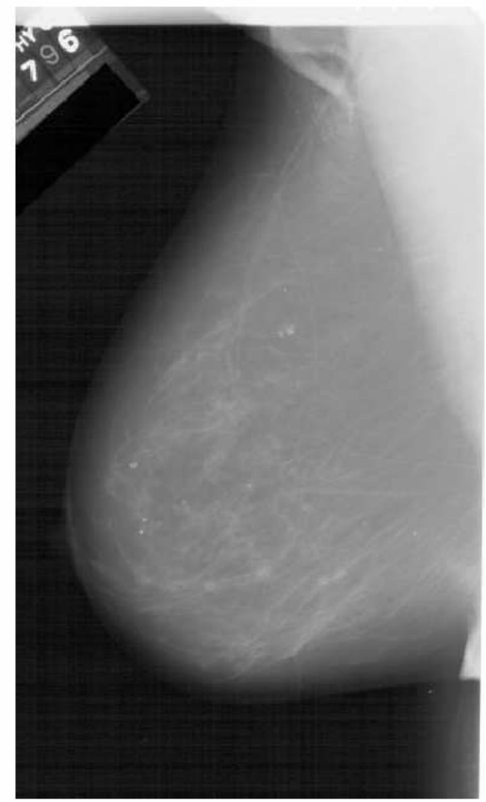

Application to digitalized mammographies

Colored Maps :

segmentation of dense $h > 0.52$ areas and fatty $h < 0.38$ areas

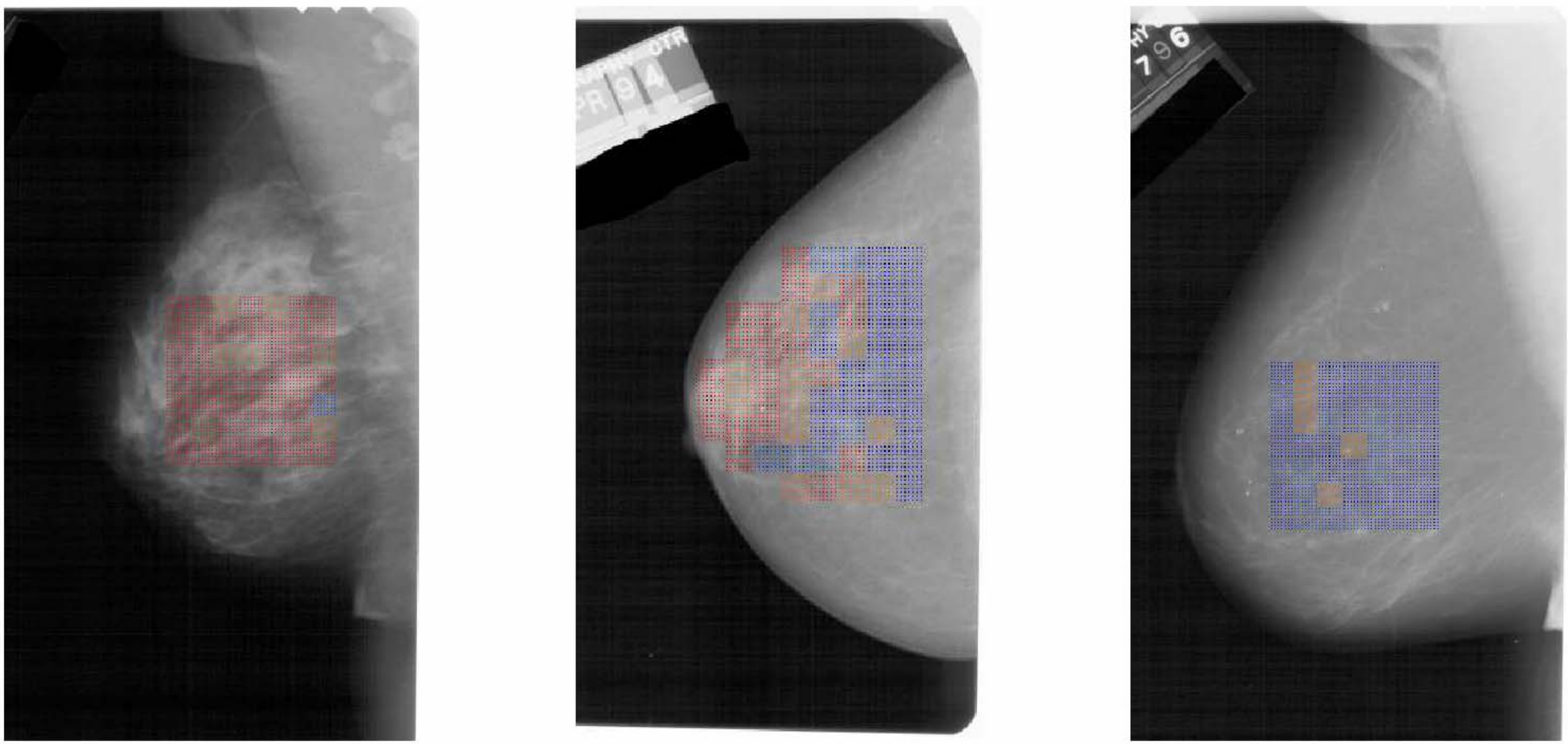

Microcalcifications detection

Segmentation of WT skeleton lines :
microcalcifications vs background texture

- Background lines
- Microcalcifications
  almost-punctual objects behave like 'Dirac' shapes ($h = -1$)

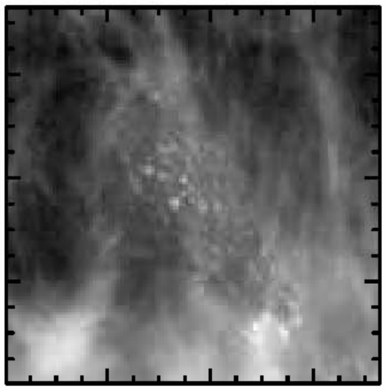

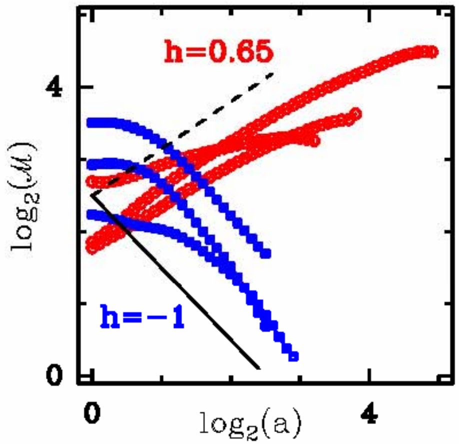

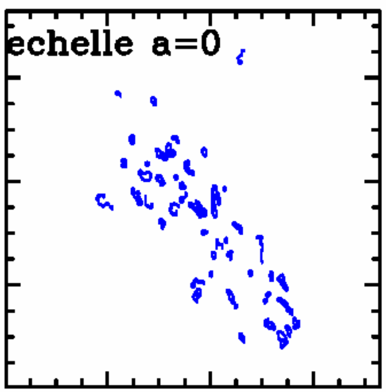

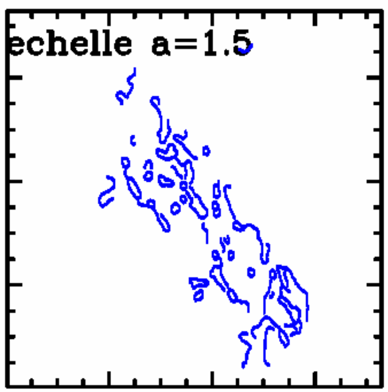

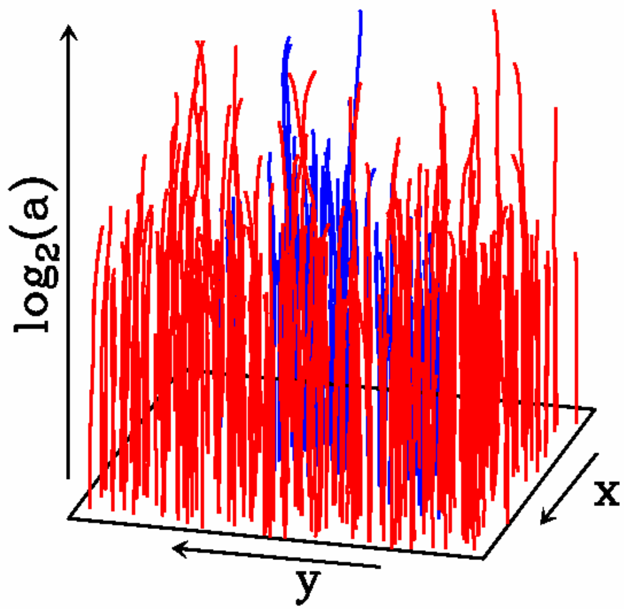

Cluster of microcalcifications

Study of microcalcification spatial distribution

Partition functions :

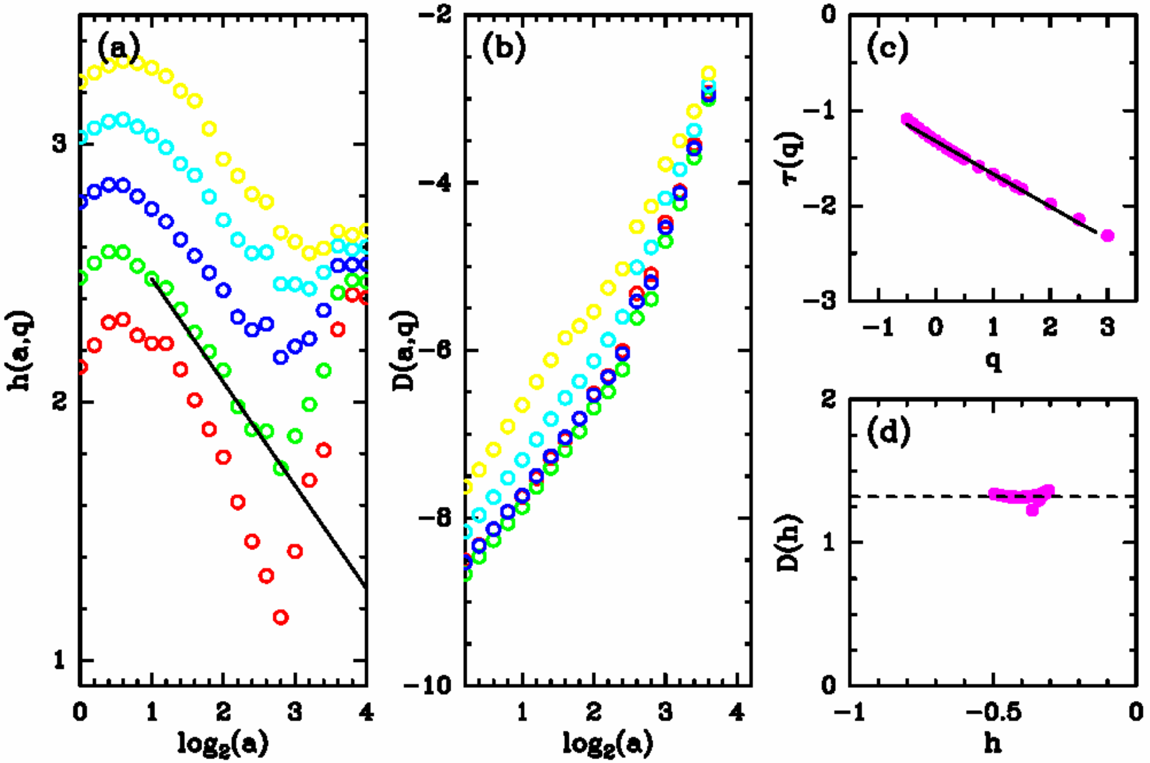

$$D_F = 1.3$$

observation :

fractal ramification of cluster of microcalcifications

$(1 < D_F < 2)$ seems to be correlated to the pathology's malignancy

Conclusions and prospects (1)

- the 2D WTMM method provides a framework for an automated measure of the breast radio-density and for studying the fractal geometry of clusters of microcalcifi cations.
- further study is necessary to validate quantitatively how far measuring the fractal dimension D_F could improve computer-aided diagnosis systems benign/malignant

3D scalar WTMM method

3D data

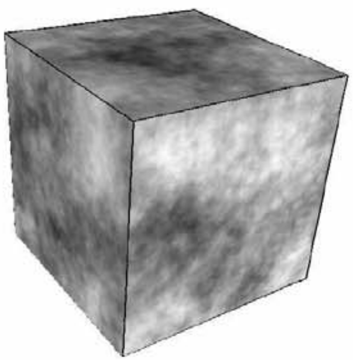

$$\underbrace{\xrightarrow{\text{Smoothing scale } a} \quad \phi_a \quad \xrightarrow{\text{Gradient } \nabla} \quad \left[\frac{\partial}{\partial x}, \frac{\partial}{\partial y}, \frac{\partial}{\partial z}\right]}_{\text{Wavelet Transform}}$$

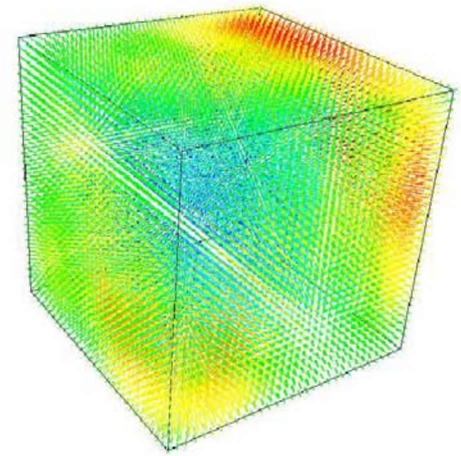

$\downarrow$

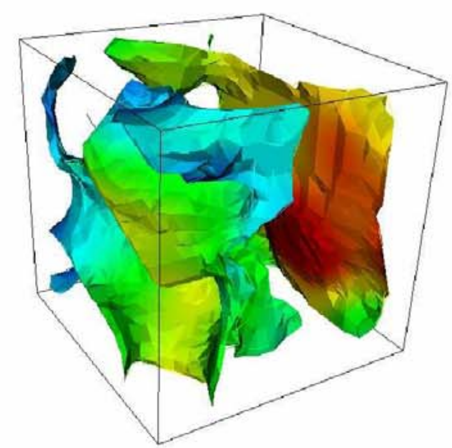

$$\mathbf{T}_{\psi}(\mathbf{r}, a) = \begin{pmatrix} I * \frac{\partial \phi_a}{\partial x}(\mathbf{r}) \\ I * \frac{\partial \phi_a}{\partial y}(\mathbf{r}) \\ I * \frac{\partial \phi_a}{\partial z}(\mathbf{r}) \end{pmatrix} = \nabla \left(I * \phi_a \right)(\mathbf{r})$$

3D scalar WTMM method : skeleton

WTMM surfaces

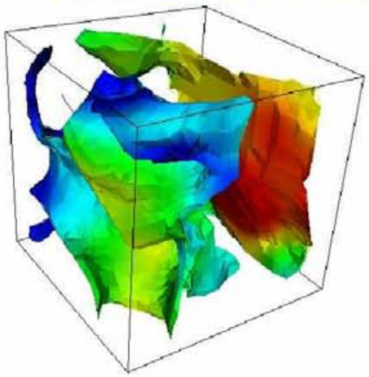

WTMM surfaces at 3 different scales

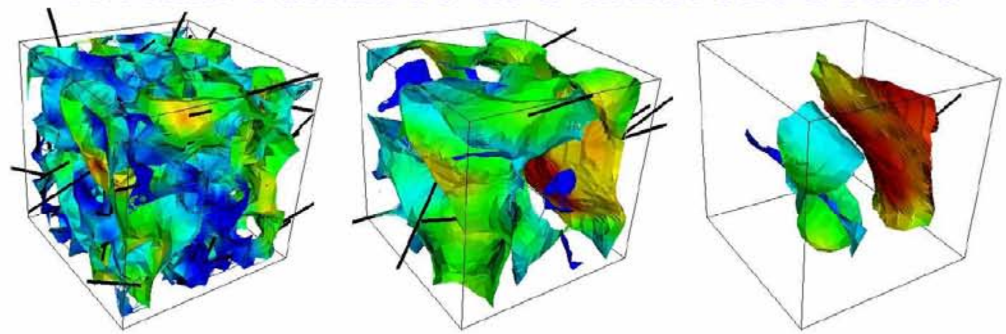

WTMMM points

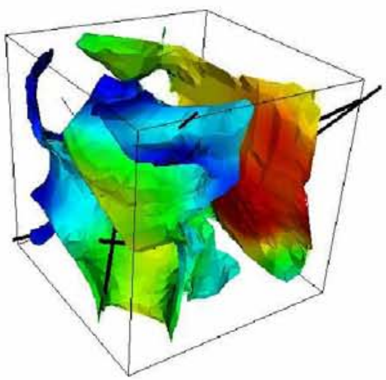

Maxima lines : WT Skeleton (projection along z)

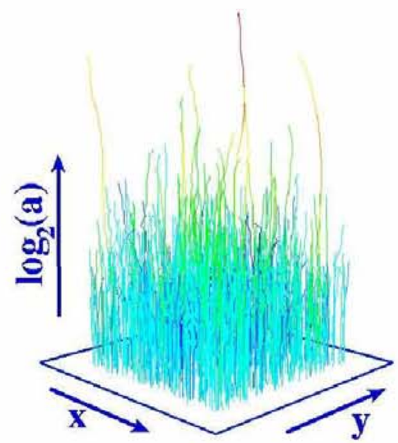

Test-application to synthetic 3D monofractal fields

fractional Brownian fields : $B_H(\mathrm{r})$

- $H < 0.5$: anti-correlated increments
- $H = 0.5$: uncorrelated increments
- $H > 0.5$: correlated increments

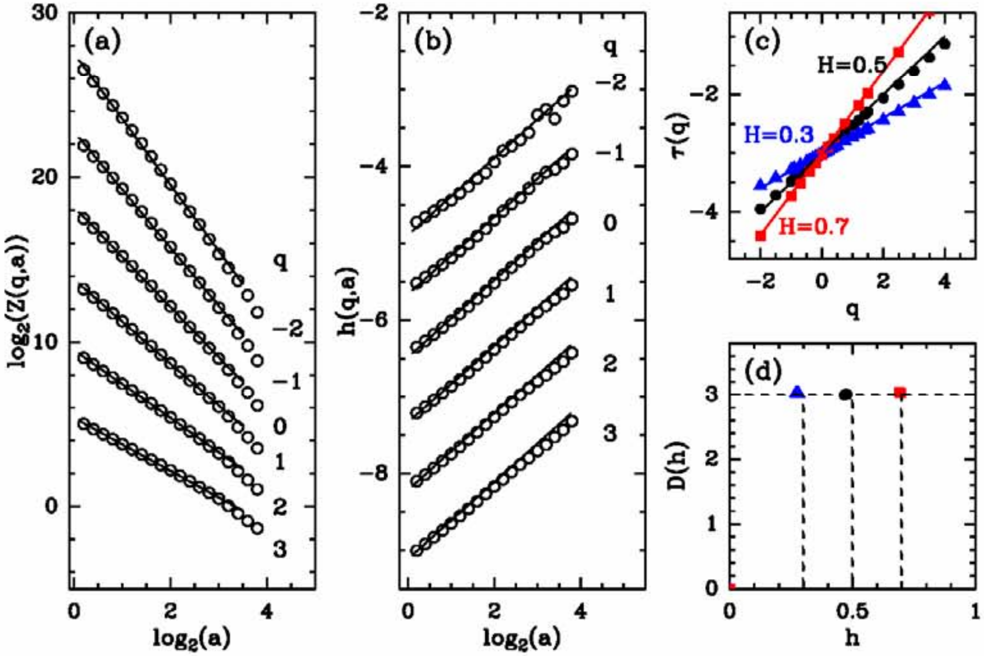

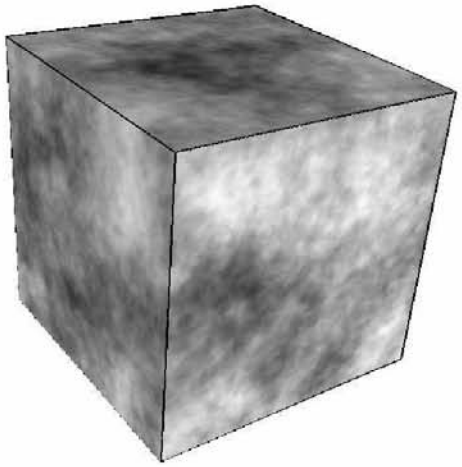

Theoretical predictions :

- $\tau(q)$ is linear:
  $\tau(q) = qH - 3$
- multifractal spectrum is degenerated:
  $D(h = H) = 3$

Test-application to synthetic 3D multifractal fields

3D **multifractal** **fields (Fractionally Integrated Singular Cascades)**

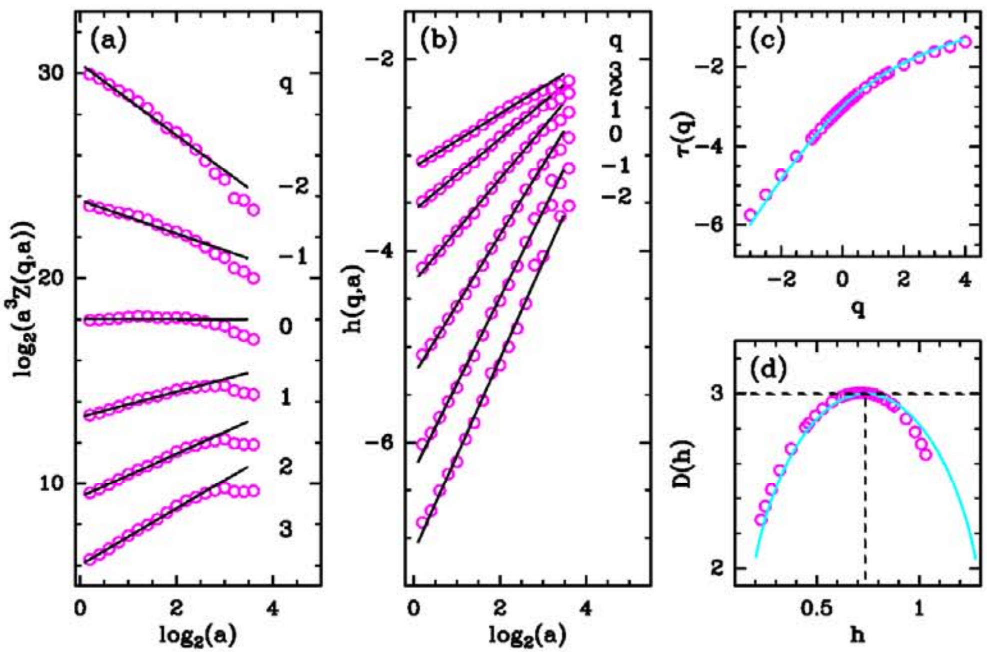

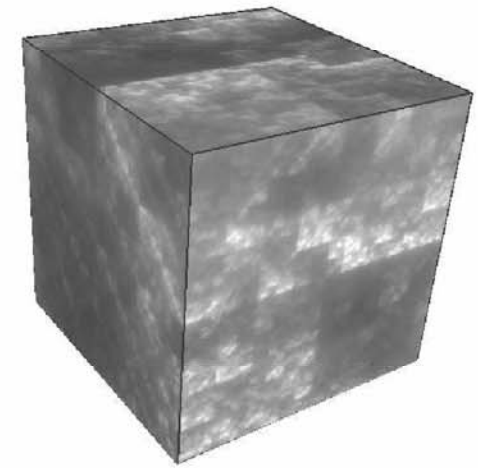

Theoretical predictions :

☞ $\tau(q) = -2 - q(1 - H^*) - \log_2(p_1{}^q + p_2{}^q).$
with $p_1 + p_2 = 1$

☞ **singularity spectrum is a non-degenerated convex curve**

3D dissipation field : isotropic turbulence DNS

pseudo-spectral code, $(512)^3$ **grid,** $R_\lambda = 216$ **(M. Meneguzzi)**

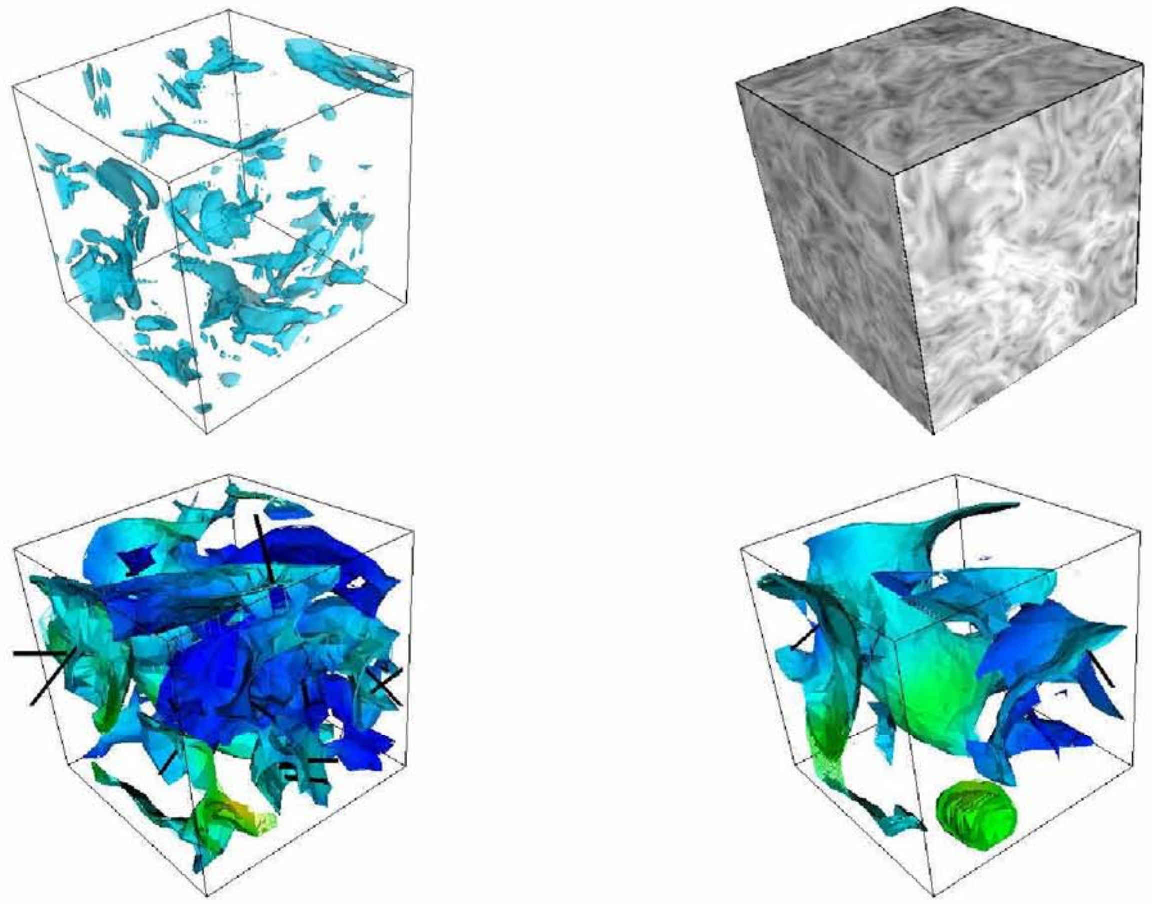

3D WTMM methodology *vs* Box-Counting algorithms

☞ "**Box-Counting**" algorithm, binomial fit with $p_1 = 0.3$ and $p_2 = 0.7$ $\rightarrow$ $\boxed{p_1 + p_2 = 1}$: diagnoses a **conservative** multiplicative structure

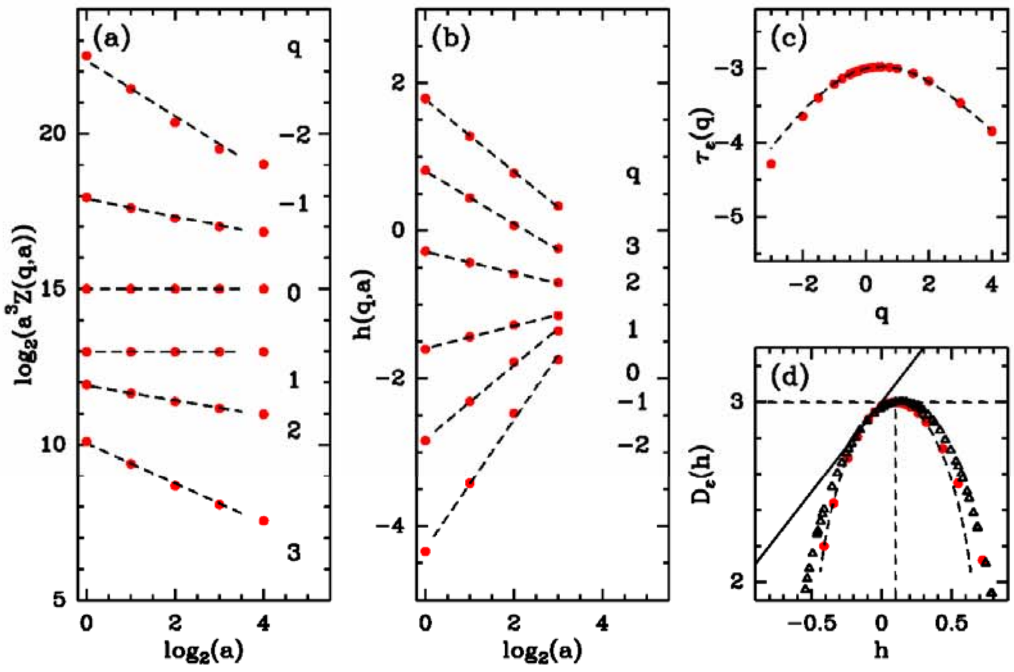

dissipation

binomial model :

$$\tau(q) = -2 - q - \log_2(p_1{}^q + p_2{}^q)$$

3D WTMM methodology *vs* Box-Counting algorithms

- “**Box-Counting**” **algorithm, binomial fit with** $p_1 = 0.3$ **and** $p_2 = 0.7$ $\rightarrow$ $\boxed{p_1 + p_2 = 1}$ **: diagnoses a conservative multiplicative structure**
- “**3D WTMM**”**method reveals a non-conservative multiplicative structure :**
  binomial fit with $p_1 = 0.36$ **and** $p_2 = 0.80$ $\Rightarrow$ $\boxed{p_1 + p_2 \neq 1}$

dissipation

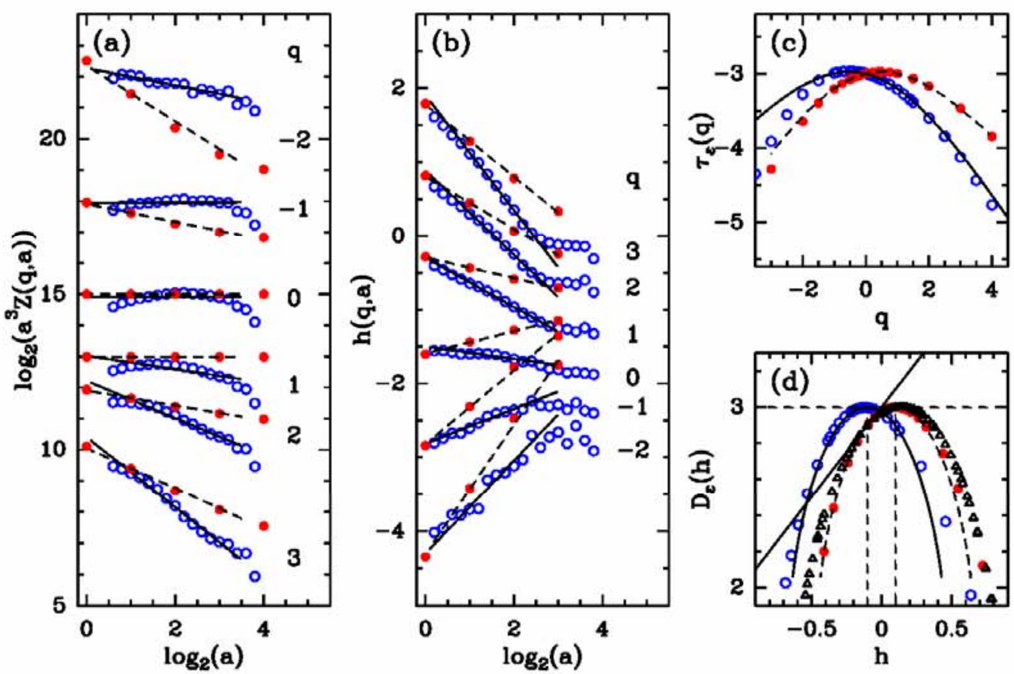

binomial model :

$$\tau(q) = -2 - q - \log_2(p_1{}^q + p_2{}^q)$$

remark:

$$p_1 = \frac{p_1}{p_1 + p_2}$$

$\Rightarrow$ inconsistent box-counting !

Self-similar multifractal vector-valued measure (2D case)

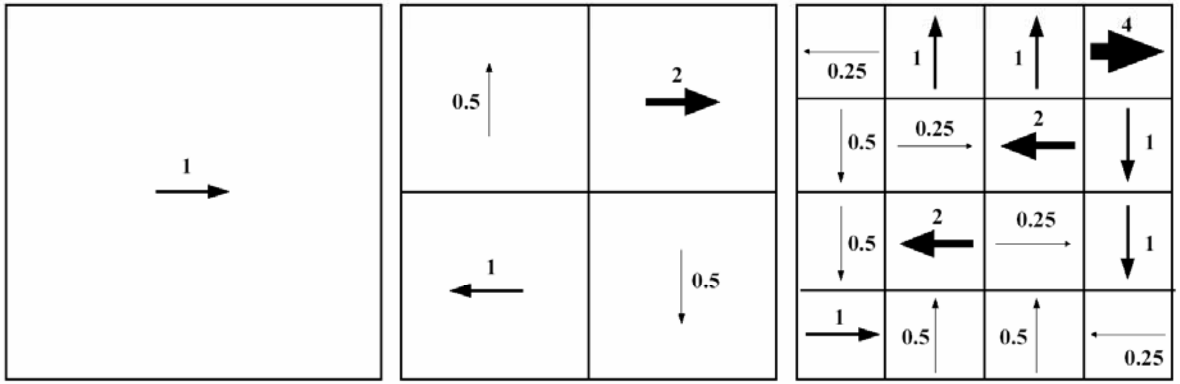

- Falconer et O'Neil (1995)
- scalar measure $\{ \mathrm{r} : \lim_{l \to 0} \frac{\log \mu(B(\mathrm{r}, l))}{\log l} = \alpha \}, \quad \alpha = h + 2$

$$\mathcal{Z}(q, l) = \sum_i \mu_i^q(l) \sim l^{\tau_\mu(q)}$$

- vector-valued measure $\left\{ \mathrm{r} : \lim_{l \to 0} \frac{\log \int_{B(\mathrm{r}, l)} ||\Phi_l \mu(\mathrm{s})|| d\mathcal{L}_d(\mathrm{s})}{\log l} = \alpha \right\}, \quad \alpha = h + 2$

$$\mathcal{Z}(q, l) = \sum_i ||\Phi_l \mu||_i^q \sim l^{\tau_\mu(q)}$$

Self-similar multifractal vector-valued measure (2D case)

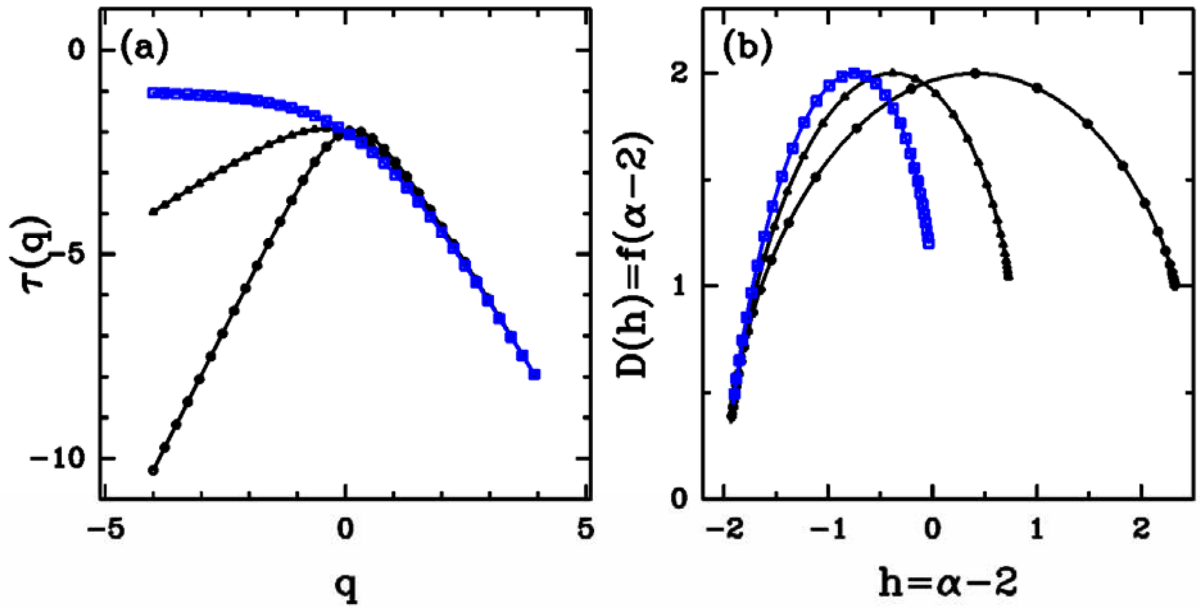

☞ $\tau_{\mu}(q) = -\frac{\log(p_1^q + p_2^q + p_3^q + p_4^q)}{\log 2}$

☞ $D_{\mu}(h) = f_{\mu}(\alpha - 2) = \inf_q (qh - \tau_{\mu}(q)).$

Tensorial wavelet transform (2D case)

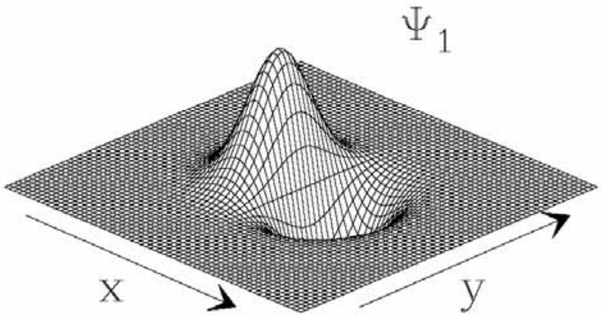

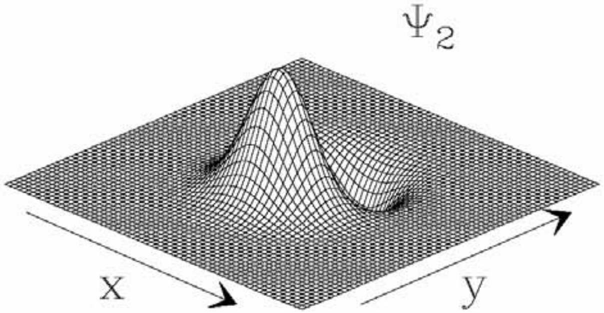

1. **Tensorial wavelet transform of field** $\mathbf{V} = (V_1, V_2)$ **:**

$$\mathbb{T}_{\psi}[\mathrm{V}](\mathrm{b}, a) = (\mathbf{T}_{\psi_i}[V_j](\mathrm{b}, a)) = \begin{pmatrix} T_{\psi_1}[V_1] & T_{\psi_1}[V_2] \\ T_{\psi_2}[V_1] & T_{\psi_2}[V_2] \end{pmatrix}$$

$$T_{\psi_i}[V_j](\mathrm{b}, a) = a^{-3} \int d^3\mathrm{r}\ \psi_i\left(a^{-1}(\mathrm{r} - \mathrm{b})\right) V_j(\mathrm{r}), j = 1, 2$$

2. **Direction of greatest variation of vector field :**

$$|\mathbb{T}_{\psi}[\mathrm{V}]| = \sup_{\mathrm{C} \neq 0} \frac{||\mathbb{T}_{\psi}[\mathrm{V}].\mathrm{C}||}{||\mathrm{C}||}$$

3. **Singular value decomposition of WT tensor:**

$$\mathbb{T}_{\psi}[\mathrm{V}] = \left(G\right) . \begin{pmatrix} \sigma_{\max} & 0 \\ 0 & \sigma_{\min} \end{pmatrix} . \left(D\right)^T$$

4. **Tensorial wavelet transform** :

$$\mathbf{T}_{\psi,\max}[\mathrm{V}](\mathrm{b}, a) = \sigma_{\max} \mathbf{G}_{\sigma_{\max}}$$

Tensorial 2D WTMM methodology

Data

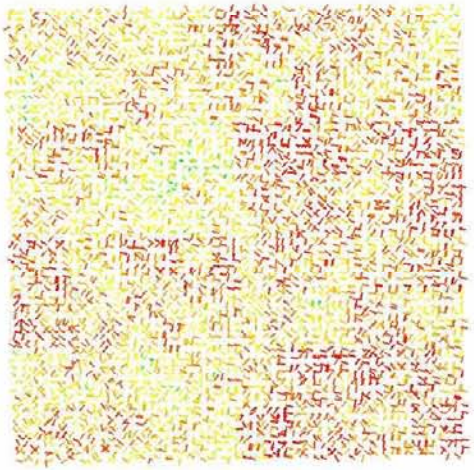

Tensorial wavelet transform

$$\mathbf{T}_{\boldsymbol{\psi},\max}[\mathbf{V}](\mathbf{b},a) = \sigma_{\max}\mathbf{G}_{\sigma_{\max}}$$

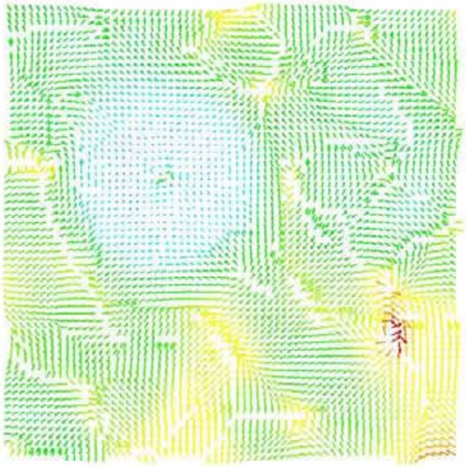

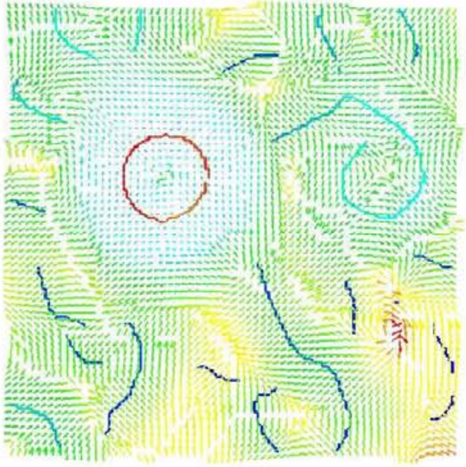

Modulus Maxima $\boldsymbol{\sigma}_{\max}$ chains of tensorial wavelet transform at scale a :

$$\left\{(b,a)/\frac{\partial\boldsymbol{\sigma}_{\max}}{\partial G_{\max}} = 0 \quad \text{et} \quad \frac{\partial^2\boldsymbol{\sigma}_{\max}}{\partial G^2_{\max}} < 0\right\}$$

Tensorial 2D WTMM methodology: Skeleton

WTMM Chains

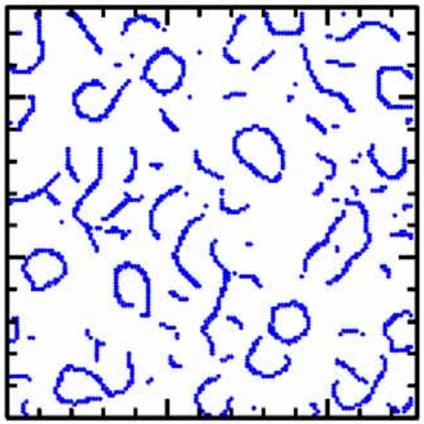

WTMMM

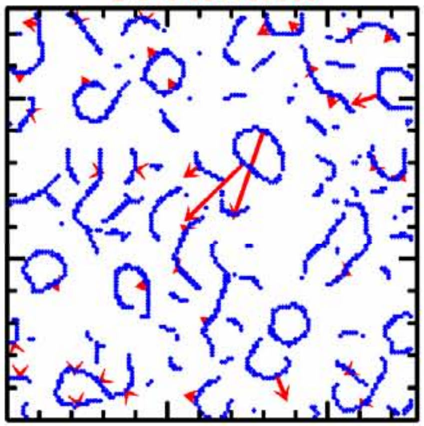

WTMM Chains at 3 different scales

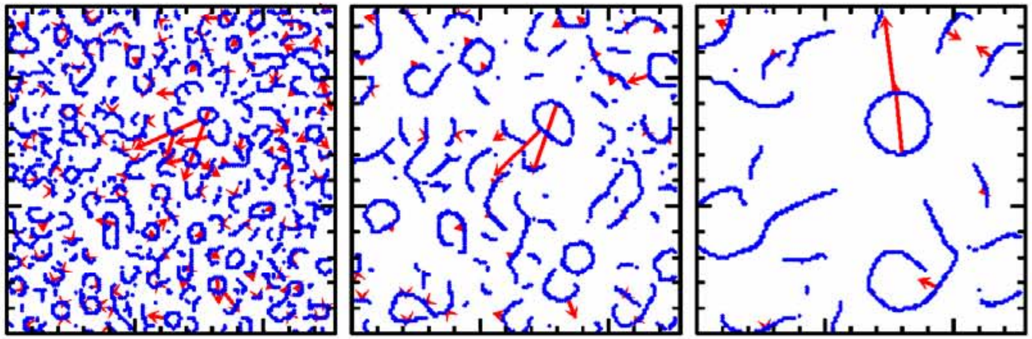

Maxima lines : WT Skeleton

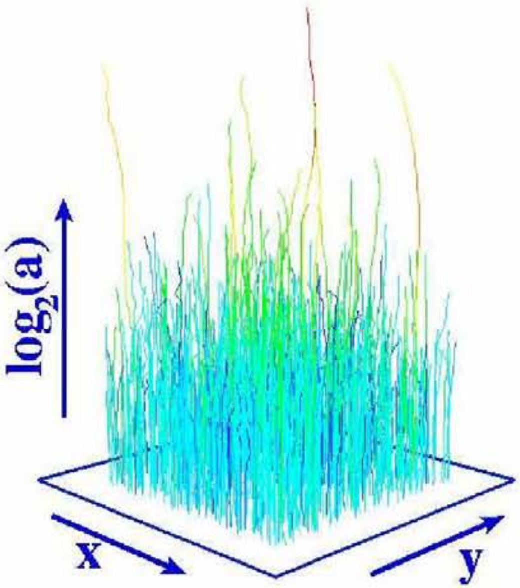

Monofractal 2D vector fields

fractional Brownian fields : $\mathrm{B}_H(\mathrm{r})$

☞ **Spectral method simulation**

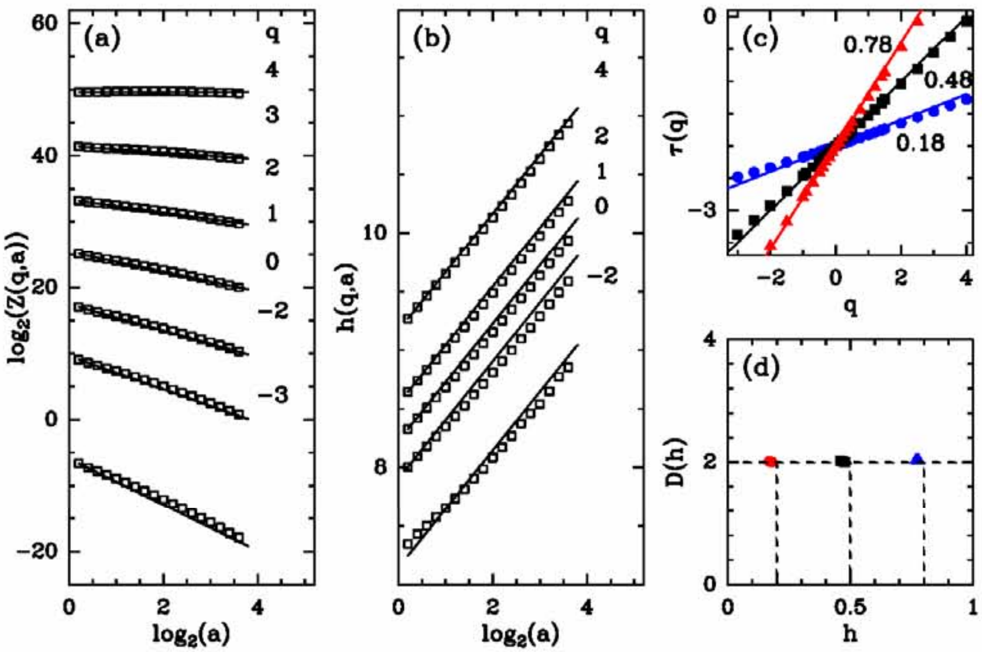

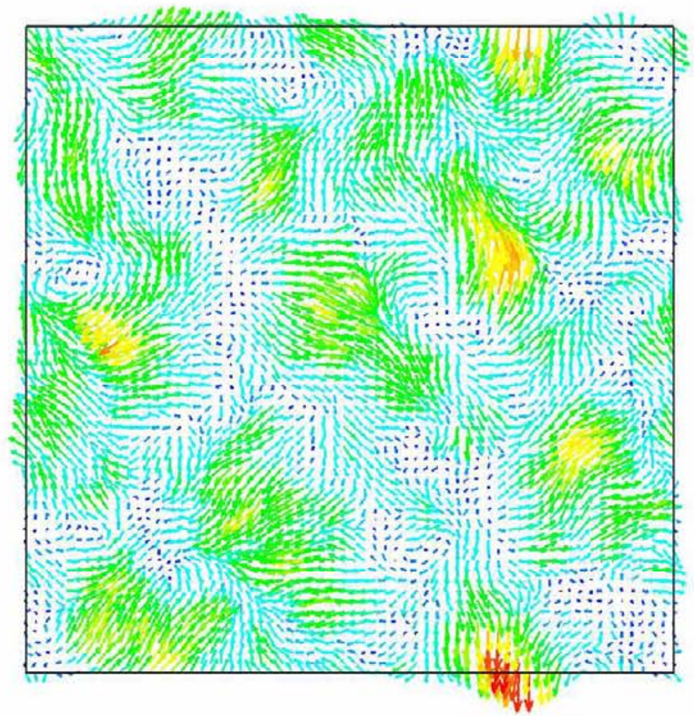

Theoretical predictions :

- linear $\tau(q)$: $\tau(q) = qH - 2$
- degenerated singularity spectrum:

$$D(h = H) = 2$$

2D self-similar multifractal vector-valued measures

Self-similar multifractal vector-valued measures
(Falconer and O'Neil's model)

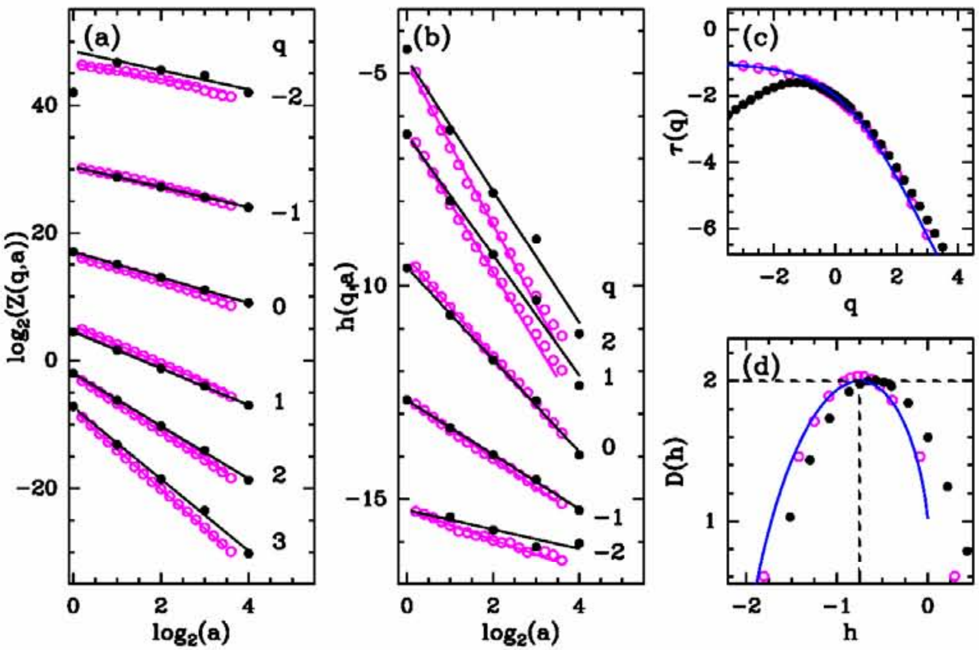

● vectorial box-counting

○ vectorial 2D WTMM method

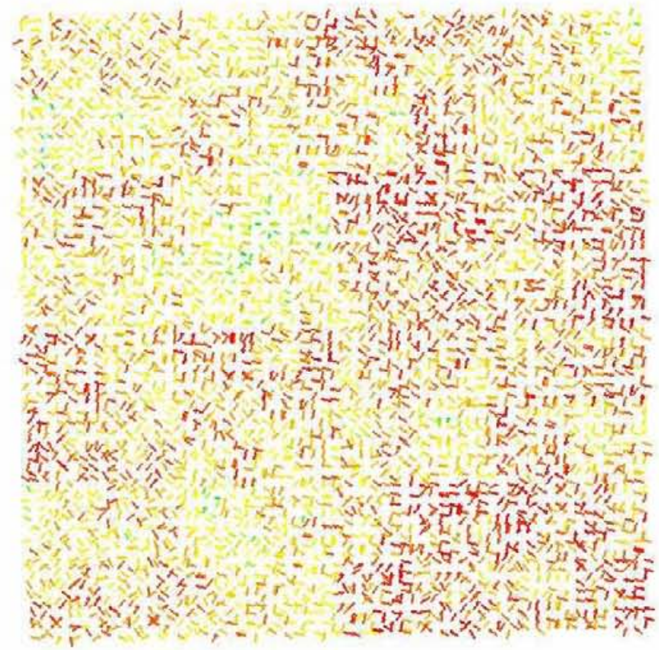

Theoretical predictions:

- $\tau(q) = -\log_2(p_1{}^q + p_2{}^q + p_3{}^q + p_4{}^q)$
  $p_1 = p_4 = 0.5$, $p_2 = 2$ and $p_3 = 1$
- **vectorial box-counting is less accurate**

Tensorial 3D WTMM method: turbulent velocity field ($R_\lambda = 140$)

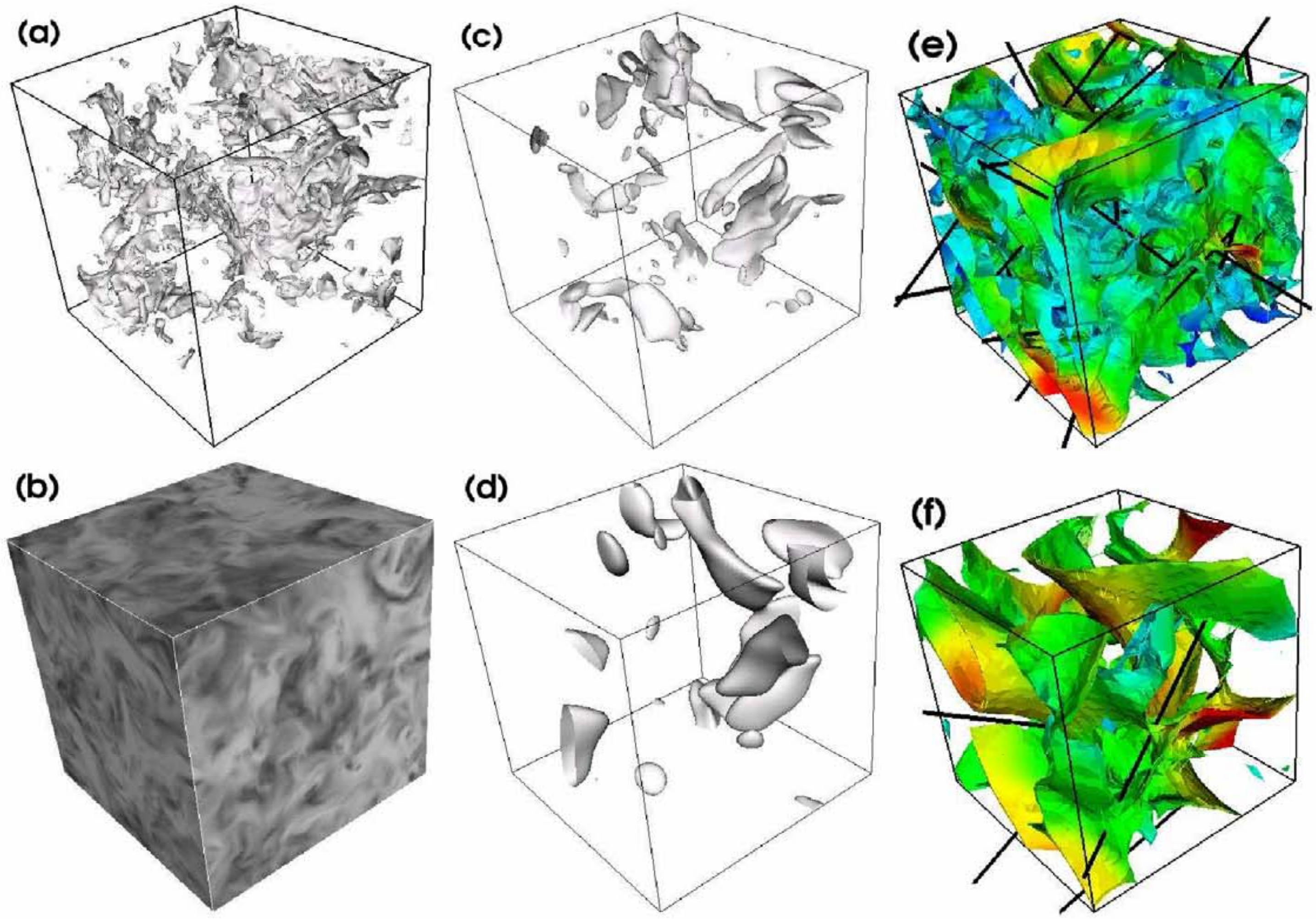

Tensorial 3D WTMM method: singularity spectrum of velocity

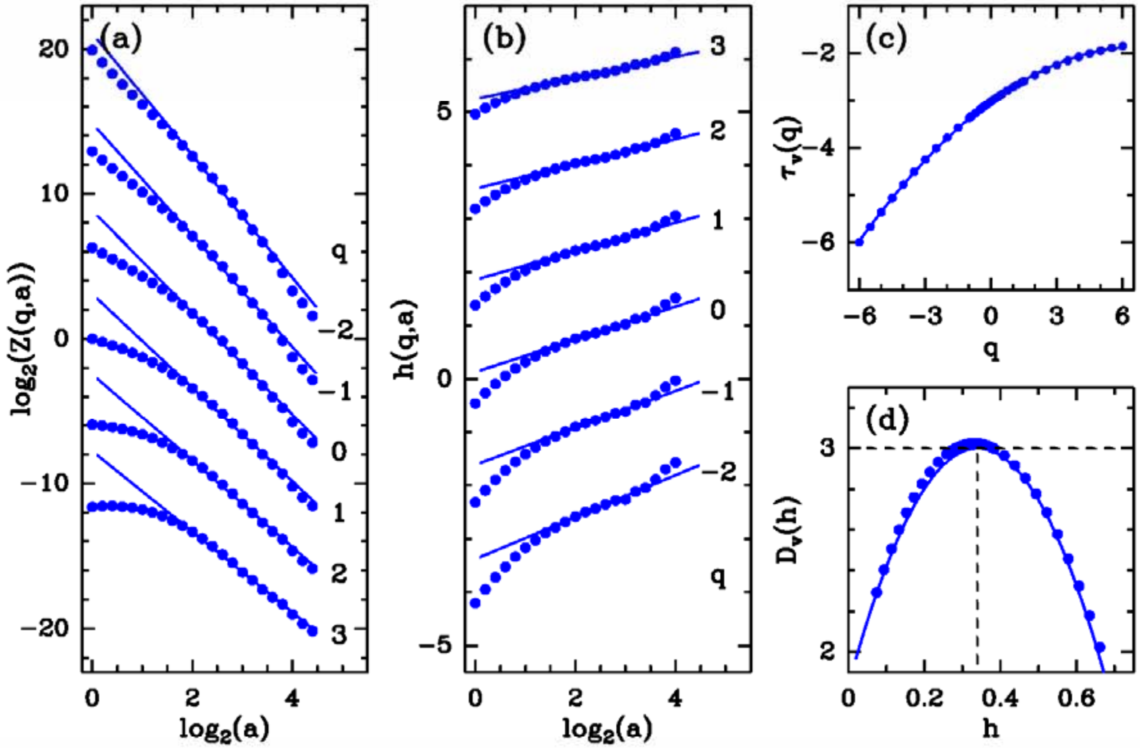

- parabolic fit: $\tau(q) = -C_0 - C_1 q - C_2 \frac{q^2}{2}$
- intermittency coefficient $C_2 = 0.049 \pm 0.004$

1D increments method:

- longitudinal : $C_2(\delta v_L) \sim 0.025$
  transverse : $C_2(\delta v_T) \sim 0.040$

Tensorial 3D WTMM method: turbulent vorticity field ($R_\lambda = 140$)

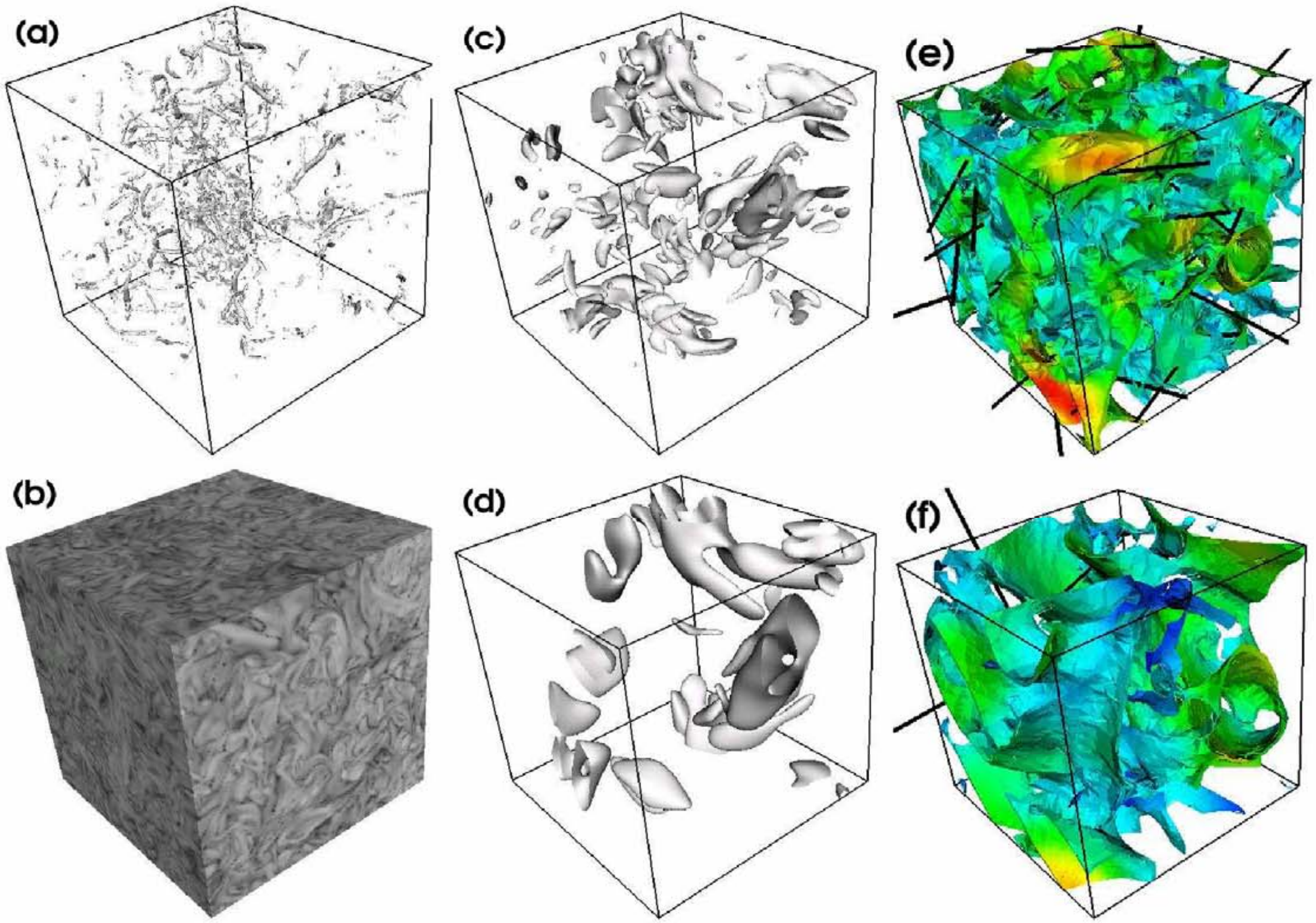

Tensorial 3D WTMM method: singularity spectrum of vorticity

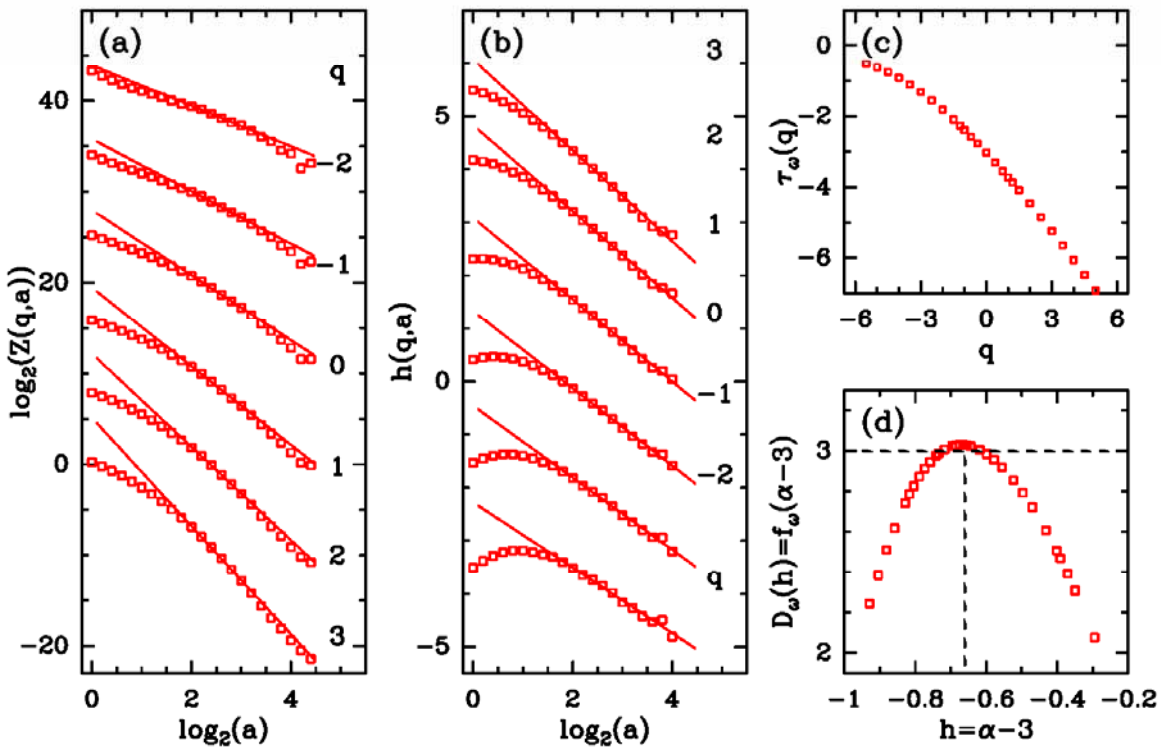

□ vorticity

Tensorial 3D WTMM method: singularity spectrum of vorticity

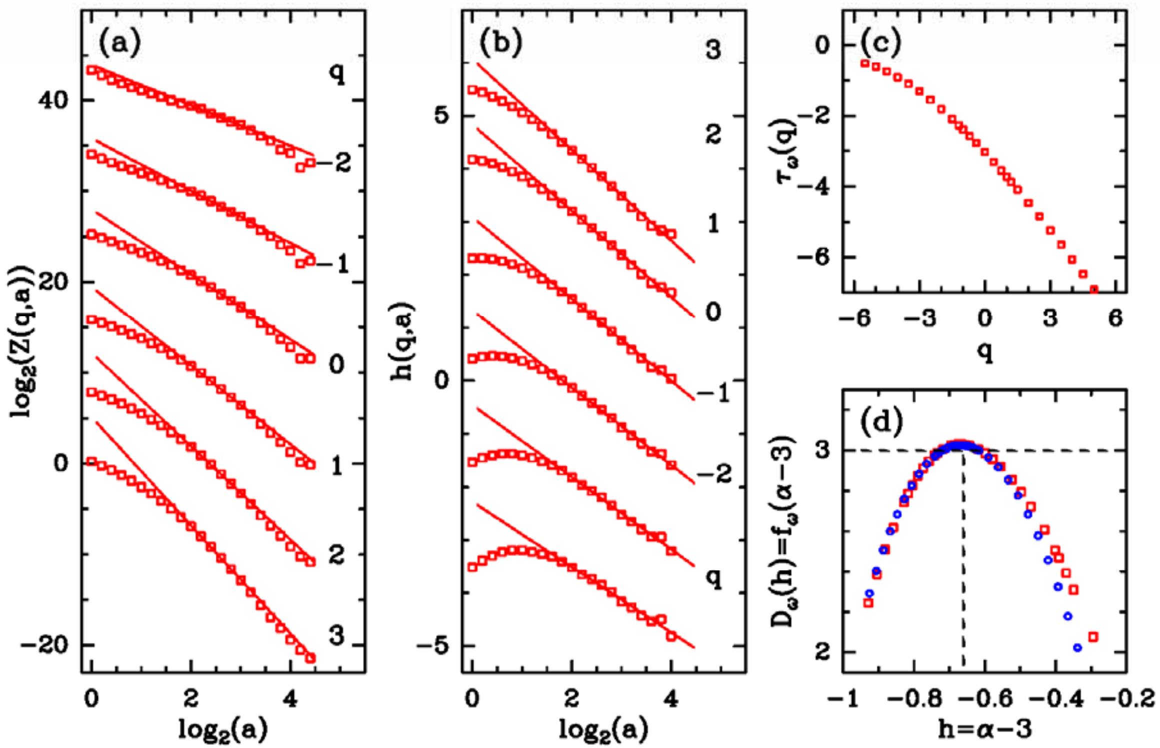

□ vorticity

○ $D_v(h+1)$ spectrum translated velocity

$\Rightarrow$ same 3D intermittency coefficient !

Conclusion

assessment:

- WTMM multifractal analysis: moving towards vector fields

outlooks :

- better understanding of the information embedded in the WT tensor.
- identification of coherent structures in turbulence using WT tensor's smallest singular value: vorticity filaments or sheets.
- others applications : astrophysics (interstellar medium, interstellar turbulence), MHD, geophysics, ...

Thanks :

- E. Lévêque, Laboratoire de Physique, ENS Lyon (Turbulent flows DNS).

PHYSICS TODAY

JANUARY 1990

References

Generalizing the wavelet-based multifractal formalism to vector-valued random fields : application to turbulent velocity and vorticity 3D numerical data.

P. KESTENER & A. ARNEODO, Phys. Rev. Lett. (2004), to appear

A wavelet-based method for multifractal analysis of 3D random fields : application to turbulence simulation data.

P. KESTENER & A. ARNEODO, in Proc. 4th Pacific Symposium on Flow visualization and Image Processing, edited by J. Prenel and Y. Bailly (2004), to appear

Three-dimensional wavelet-based multifractal method : the need for revisiting the multifractal description of turbulence dissipation data.

P. KESTENER & A. ARNEODO, Phys. Rev. Lett. **91**, 194501 (2003)

A wavelet-based method for multifractal image analysis : from theoretical concepts to experimental applications.

A. ARNEODO, N. DECOSTER, P. KESTENER & S.G. ROUX, Advances in Imaging and Electron Physics **126**, 1 (2003)

Wavelet-based multifractal formalism to assist in diagnosis in digitized mamograms.

P. KESTENER, J.M. LINA, P. SAINT-JEAN & A. ARNEODO, Image Anal. Stereol. **20**, 169 (2001)

A wavelet-based method for multifractal image analysis. I. Methodology and test applications on isotropic rough surfaces.

A. ARNEODO, N. DECOSTER & S.G. ROUX, Eur. Phys. J. B **15**, 567 (2000)

A wavelet-based method for multifractal image analysis. II. Application to synthetic multifractal rough surfaces.

N. DECOSTER, S.G. ROUX & A. ARNEODO, Eur. Phys. J. B **15**, 739 (2000)

A wavelet-based method for multifractal image analysis. III. Application to high resolution satellite images of cloud structure.

A. ARNEODO, S.G. ROUX & N. DECOSTER, Eur. Phys. J. B **15**, 765 (2000)

Intermittency, log-normal statistics and multifractal cascade process in high-resolution stallite images of cloud structure.

A. ARNEODO, N. DECOSTER & S.G. ROUX, Phys. Rev. Lett. **83**, 1255 (1999)